Energy Reports 15 (2026) 108888

Contents lists available at ScienceDirect

Energy Reports

journal homepage: www.elsevier.com/locate/egyr

Research paper

Environmental benefits and impacts forecasting for three-phase induction motors operations in marine applications: A multiple linear regression approach

Antonino D'Amico *, Sonia Longo, Maurizio Cellura, Massimo Caruso, Rosario Miceli

Department of Engineering, University of Palermo, Viale delle Scienze Building 9, Palermo 90128, Italy

A R T I C L E I N F O

Keywords:
LCA
Environmental benefits
Ship powertrains
Power losses minimization algorithm
Forecasting method
Multiple linear regression

A B S T R A C T

In a world characterized by unsustainable production and consumption paths, it is crucial to conceptualize and implement eco-friendly strategies to achieve the set decarbonization goals. Maritime transport, mainly characterised by fossil fuels-based powertrains, is responsible for 2.89 % of anthropogenic greenhouse gas emissions, for 15 % of global NO_x emissions and 13 % of SO_x, resulting a critical sector in which to promote sustainable strategies. Despite the direct environmental impacts are negligible during the operative phase in a full electric vessel, the impacts related to the electricity production are not negligible, so more efficient propulsion system management is still important. A better management can be achieved using control algorithms capable of reducing energy consumption under specific motor operating conditions. However, the real induced environmental benefits must be calculated along the entire energy supply chain. Through a life cycle assessment, this work aims at a dual objective. First, it aims to evaluate the environmental benefits obtainable by applying a power loss minimization algorithm to a three-phase induction motor compared to traditional field-oriented control algorithms under different working conditions. The optimized algorithm reduces all environmental impacts by approximately 15 %. A scenario analysis, based on different electricity production processes, highlights that the sustainability of electric powertrains increases by improving the share of renewable electricity in the production mix. Secondly, to simplify life cycle assessment computational burdens, an early design model based on multiple linear regression methods is proposed as a simple and reliable alternative ($R^2 \simeq 98$ %) to support the decision-maker in the preliminary planning phase.

1. Introduction

Current production and consumption models produce unsustainable impacts on a global scale. The excessive use of raw materials and energy, the degradation of soil and natural habitats, and the emissions of polluting substances are altering ecosystems and compromising the "health" of the planet. It is therefore necessary to modify the current approach to production and consumption by reversing the current trends, which constitute a serious threat not only to the environment but also to the economic and social well-being of communities, by encouraging the spread of sustainable production and consumption. This change is fundamental to achieve a decoupling between economic growth and environmental degradation and to allow populations to satisfy their needs. As part of the definition of sustainable production and consumption strategies, it is necessary to apply methodologies for analysing the energy-environmental performance of products throughout their entire life cycle, from which to draw effective indications for improving environmental performance. In this regard, maritime transport represents a sector in which to act decisively, proposing technological and optimization solutions to achieve the decarbonization objectives introduced with the Paris Agreement on climate change (UN, 2015) and updated in subsequent Conferences of the Parties (COP) such as COP26 (United Nations Framework Convention on Climate Finance, 2021) in Glasgow, COP27 in Sharm el-Sheikh (United Nations Framework Convention on Climate Finance, 2022) and COP28 held in Dubai in 2023 (United Nations Framework Convention on Climate Finance, 2024). Maritime transport, indeed, covers approximately 90 % of global trade, representing a large portion of the world economy (Gu et al., 2019). However, due to mechanical propulsion

* Corresponding author.
E-mail addresses: antonino.damico01@unipa.it (A. D'Amico), sonia.longo@unipa.it (S. Longo), maurizio.cellura@unipa.it (M. Cellura), massimo.caruso16@unipa.it (M. Caruso), rosario.miceli@unipa.it (R. Miceli).

https://doi.org/10.1016/j.egyr.2025.12.025
Received 27 June 2025; Received in revised form 8 November 2025; Accepted 6 December 2025
Available online 13 December 2025

Nomenclatures

Acronyms

CNMS	Centro Nazionale per la Mobilità Sostenibile
FOC	Field-Oriented Control
FU	Functional Unit
HFO	Heavy Fuel Oil
IM	Induction Motor
IMO	The International Maritime Organization
LCA	Life Cycle Assessment
LHV	Lower Heating Value
LMA	Power Losses Minimization Algorithm
MGO	Heavy Fuel Oil
MLR	Multiple Linear Regression
WTW	Well-to-Wake

Environmental impact parameters

AP	Acidification Potential
ADPe	Abiotic Depletion Potential for minerals and metals
ADPf	Abiotic Depletion Potential for fossil resources
EP	Eutrophication Potential
GWP	Global warming potential
ODP	Ozone Depletion Potential
POCP	Photochemical Ozone Creation Potential
WDP	Water deprivation potential

Error and performance parameters

MAPE	Mean Absolute Percentage Error
RMSE	Root Mean Square Error
R^2	Determination Coefficient

Motor parameters

Load	Load Torque [Nm]
Ψ	Magnetizing flux [Wb]
ω_{ref}	Rotor speed [rad/s] (1 rad/s = 9.55 rpm)

systems powered by conventional fuels, such as heavy fuel oil (HFO), marine gas oil (MGO), diesel or oil, naval mobility represents one of the main factors contributing to air pollution (Lu et al., 2020) and global warming (Monteiro et al., 2018). The shipping industry is responsible for approximately 15 % of global NOx emissions and 13 % of SOx (Sui et al., 2020), and if current systems are maintained, polluting emissions are expected to increase by 150–250 % in the coming decades (Bouman et al., 2017). Today, thanks also to the work of the International Maritime Organization (IMO) (IMO, 2024), global environmental regulations are in place to decarbonize long and short-range maritime shipping, through the replacement of conventional propulsion systems with eco-compatible propulsion systems (Bach et al., 2020). Ships' electrification represents an actual and important research topic and it is one of the proposed solutions for achieving the objective of carbon neutrality in the short-range naval mobility sector (Kim et al., 2022; Perčić et al., 2022). Some researchers focus on evaluating the environmental benefits of electric propulsion. For example, in (Jeong et al., 2022), the real environmental sustainability of naval electric propulsion is investigated, with a life cycle thinking approach, through comparative analyses between diesel and battery-electric propulsion extended to different sources of electrical energy. In (Wang et al., 2021) and (Ammar and Seddiek, 2021) the results of a life cycle assessment and life cycle costing assessment of some electric propulsion systems are presented, evaluating their degree of sustainability achieved; the first evaluates a battery-powered electric propulsion system installed on a ferry while the second evaluates diesel electric and combined gas turbine electric and steam systems on a passenger ship. In other cases, the research focuses on ship's electrical power system (Kim and Jeon, 2022) and still others on its energy management and optimization (Wu et al., 2020; Zahedi et al., 2014). It is possible to find three different types of electric boats on the market, such as hybrid ship, plug-in hybrid ship and fully electric ship (Solutions, 2021). While the first two versions of the electric vessel have an internal combustion motor and an electric battery, charged through excess energy from the motor (hybrid ship version) (Dedes et al., 2012) or from the electricity grid (plug-in hybrid ship) (Jianyun et al., 2019), the fully electric version uses only the electrical energy stored in a battery using the electricity grid and eliminates exhaust emissions during the ship operational phase (Gagatsi et al., 2016). The life cycle environmental analysis must include not only emissions related to direct activities such as fuel combustion in a ship motor or energy consumption for shipbuilding, but also embodied emissions over the entire life cycle (Blanco-Davis and Zhou, 2014; DNV, 2019). Furthermore, the impacts generated in a fully electric ship are mostly attributable upstream of the operational phase, *i.e.*, in all those operations falling within the well-to-tank boundaries, as well as influenced by the production process of the consumed electrical energy and by the used energy source (Hemez et al., 2020; Perčić et al., 2023; Vakili and Ölçer, 2023). However, although negligible, it is still possible to influence the emissions attributable to the operational phase also through efficient management of the electric propulsion system. Indeed, a more efficient electric propulsion system consumes less energy under the same operating conditions, and a lower consumption of electricity leads to a consequent reduction in the environmental impacts generated by the fuel path. Therefore, the life cycle assessment application in maritime transport is essential to obtain a reliable and non-misleading estimate of environmental impacts.

Based on these premises, the research developed here represents one of the first studies at an international level on the evaluation of the environmental benefits deriving from the optimization of three-phase induction motor control techniques used in the field of naval electrification. In fact, from an in-depth and careful check of the state of the art carried out through consultation of the main international ISI journals, few Life Cycle Assessment (LCA) studies on maritime electric mobility emerged (Hemez et al., 2020; Perčić et al., 2023; Vakili and Ölçer, 2023) and no experience has been found relating to the environmental consequences deriving from the applications of motor control and optimization algorithms. Specifically, through the application of the LCA methodology, this research work has a dual objective. First of all, aims to identify the environmental benefits achieved during the operative phase of a three-phase induction motor that uses a new power losses minimization algorithm (LMA) compared to those obtained from a traditional field-oriented control (FOC) algorithm under different working conditions. Furthermore, to highlight the influence of the upstream energy source, a scenario analysis was conducted in which the effects of 5 different electrical energy paths were evaluated. The results obtained in this first phase of the work will represent a useful dataset for evaluating the potential environmental impacts avoided by hypothesizing real scenarios in which the operational phase is characterized by fixed navigation conditions (navigation times, rotor speed and resistant torque).

Secondly, it is known that the environmental assessment along the product value chain is quite complex and presents high computational costs due to the large amount of data to be collected and design choices that an expert operator must make in each single phase of the calculation procedure. In general, the environmental performance assessment of a product or service occurs through the application of the LCA calculation methodology in compliance with the international standards of the ISO 14040 series (International Organization for Standardization (ISO), 2020), to estimate the impacts according to a cradle to grave approach.

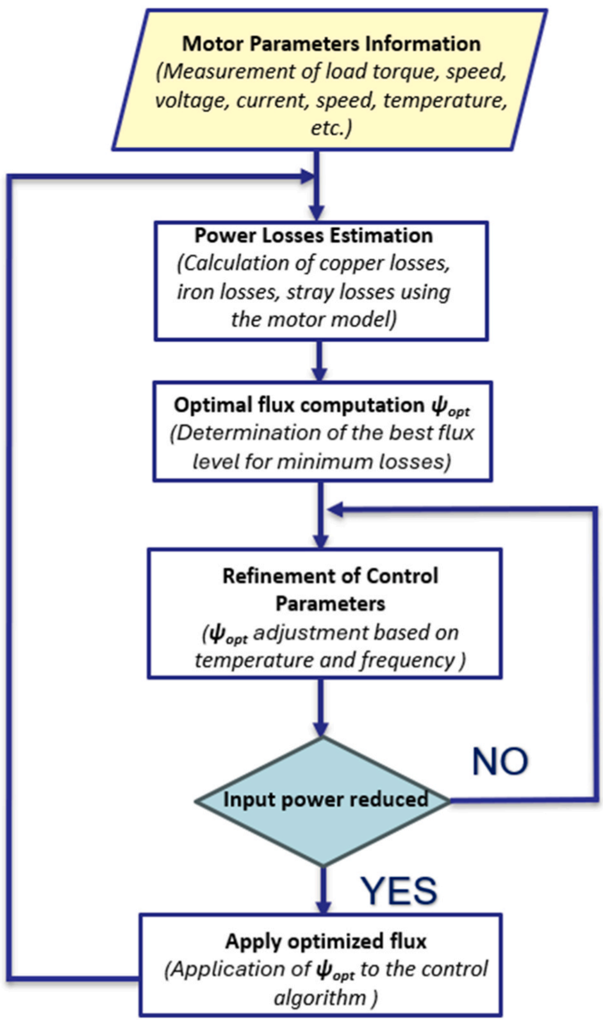

Fig. 1. Power loss minimization algorithm flowchart.

For accurate environmental planning, also during the operational phase of an electric motor in naval applications, it may be necessary to explore alternative methods to support technicians in their efforts to improve the achievable environmental performance, but also to reduce computational times. Several black box forecasting approaches, *i.e.*, based on a function deduced from samples of relevant data and describing the behaviour of the investigated system, have been applied to different problems and sectors (Ciulla et al., 2016; D'Amico et al., 2019). One of the most well-known is certainly represented by multiple linear regression (MLR) (Ciulla and D'Amico, 2019). One of the proven advantages is certainly its ease of use that makes it suitable for use even by a non-expert user (Aydinalp-Koksal and Ugursal, 2008). In the literature, it is possible to find some studies in which MLR predictive models for the evaluation of environmental impacts are developed following a life cycle assessment, but none in general applied to the mobility sector and specifically to electric motors. For example, in (Hansen et al., 2025), an estimate of the GWP100 is carried out through linear regression techniques with acceptable results ($R^2 = 0.74$) for the dairy sector. In (Ng et al., 2024), the authors aim to develop an integrated LCA-MLR framework to establish hotspot-oriented regression models in the green office buildings sector, while in (Tajuddeen et al., 2023), the authors develop machine learning models, including MLR techniques, capable of predicting the GWP of thermal insulation materials for buildings.

In this research work, for the first time applied to the electric mobility sector, the multiple linear regression method has allowed to develop simple relationships capable of determining accurately and reliably the environmental impacts generated during the operational phase of an electric motor.

Table 1
Main Rated Values and Parameters of the three-phase induction motor under test (Bruno et al., 2021).

Characteristics	Unit	Value
Power	kW	5.5
Voltage	V	400
Current	A	13
Frequency	Hz	50
Load Torque	Nm	18
Rater Speed	rpm	2850
Stator resistance	Ω	0.56
Rotor resistance	Ω	0.77
Stator inductance	H	0.116
Rotor inductance	H	0.119
k_1	Ω s	2.75
k_2	Ω s^2	0.141
Rated rotor flux	Wb	0.7

2. Materials and methods

2.1. Power loss minimization algorithm

A power loss minimization algorithm can be generally defined as a control strategy adequately designed to optimize the efficiency of an electric motor by minimizing the power losses involved in the system while ensuring adequate torque production and dynamic performance for any conditions of operation of the drive. These algorithms adjust motor control parameters (such as flux level, voltage, or slip frequency) to operate in the most energy-efficient way, leading to lower energy consumption, reduced heat generation, and enhanced operational efficiency under different load and speed conditions of the motor. Indeed, the highest efficiency of an electric motor is typically achieved near its rated operating conditions; however, under different load or speed values, efficiency can decrease significantly. To overcome this issue, power losses can be minimized through the LMA, so that efficiency can be noticeably improved under any condition. Specifically, the algorithm adopted for this work was developed in (Bruno et al., 2021) and uses a loss model-based approach for power loss minimization in induction motor (IM) drives, relying on a mathematical representation of the motor's loss components, such as iron and copper losses, including additional and stray losses. By defining the magnetizing flux ψ as the loss variable, the mathematical equation that minimizes the power losses can be obtained as a function of mechanical load and required speed. Therefore, the optimal flux value, ψ_{opt}, which strictly varies depending on the operating conditions, is applied to the motor to achieve the most energy-efficient operation. By dynamically adjusting the motor flux, the drive can minimize losses while maintaining the required torque.

The flowchart of the proposed algorithm is depicted in Fig. 1. The first step involves measuring critical motor parameters such as voltage, current, speed, load torque and temperature, serving as inputs for subsequent computations. Then, the power losses are estimated based on a predefined motor model and the optimal flux level ψ_{opt} is consequently determined. The next phase involves further refining the loss variable to optimize motor efficiency in the case of parameter variations such as temperature fluctuations and resistance changes, ensuring the accuracy over time. Finally, ψ_{opt} is applied to the control system of the motor, so it can operate at maximum efficiency. This iterative approach enables the motor system to dynamically respond to changing conditions in terms of both load and speed, ultimately minimizing power losses through the adjustment of the magnetizing flux.

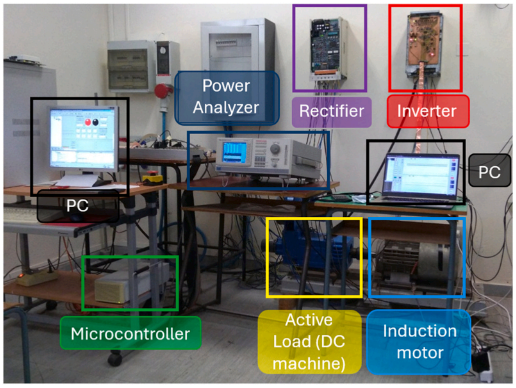

Fig. 2. Experimental test bench set up at the Electrical Drive Applications Laboratory (EDALab), University of Palermo, Italy.

2.2. Application of LCA methodology

The LCA methodology allows determining the energy and environmental impacts of the studied product in terms of consumption of resources and emissions into the environment, as well as waste production, from a life cycle perspective.

2.2.1. Goal and scope definition

In this research work, following the international standards of the ISO 14040 series (International Organization for Standardization (ISO), 2020), the LCA methodology has been applied to quantify the actual environmental performance improvement achievable by optimizing the control of a three-phase induction electric motor during its operational phase for naval applications. Particularly, the power loss minimization algorithm explained in Fig. 1 was used to replace a traditional field-oriented control system. The LMA algorithm was applied to a 5.5 kW three-phase induction motor with a double squirrel-cage rotor characterized by the nominal parameters shown in Table 1.

The motor is set up on a test bench at the Electrical Drives Applications Laboratory (EDALab), University of Palermo, Italy (Fig. 2) (Bruno et al., 2021).

In this way, Bruno et al. (2021) were able to determine the achievable energy savings by evaluating the motor input power for both algorithms by varying the motor operating conditions. In particular, the motor load torque and the rotor speed are varied. The rotor speed varied from 50 to 300 rad/s (corresponding to approximately 480–2865 rpm) with a step of 50 rad/s, while, for each speed, the load torque varied from 0 to approximately 20 Nm with an approximate step of 0.5 Nm. The input powers constitute the input data for the performed environmental analysis. Based on these data, the achievable environmental benefits that can be obtained by replacing the control algorithm (from FOC to LMA algorithm) have been calculated. Furthermore, to demonstrate the influence of the electricity generation process and the upstream energy source on the environmental sustainability of electric propulsion systems, the authors conducted a scenario analysis on 5 different electricity paths (Scenarios):

1. Electricity produced by the Italian energy mix;
2. Electricity produced by the European energy mix;
3. Electricity produced by photovoltaic systems;
4. Electricity produced by a thermoelectric power plant powered by fuel oil; and
5. Electricity produced by diesel-electric generators for a fishing vessel.

However, the scenarios that refer to energy mixes (Scenario 1 and Scenario 2) are considered the most realistic for the reference context assumed in the analysis.

According to the specifications indicated in the LCA guidelines developed by the IMO, the analysis conducted follows the "Well-to-Wake" (WTW) approach, which extends the analysis to the fuel life cycle, from fuel production to the gas exhaust system. The system boundaries determine the process units that must be included in the LCA study and in this work are:

– Electricity production; and
– Motor operating phase, varying the load torque and rotor speed.

The construction, maintenance and end-of-life phases of the motor were excluded from the analysis because the study wants to evaluate the effects in terms of missed environmental impacts obtainable by the optimization of motor efficiency through the LMA algorithm. A substantial equivalence is assumed between the life cycle phases excluded from the system boundaries whether the motor operates with the FOC algorithm or is regulated by the LMA algorithm. Concerning the environmental aspects of the investigated technology, the guidelines for the Environmental Product Declaration of the Swedish Environmental Council rules (International EPD System, 2025) were followed. This method enables the calculation of eight environmental impact categories representing the core environmental impact indicators of the International Standard EN 15804:2019 (The European Committee for Standardization (CEN), (2019)). The selected impact categories and the related characterization factors ensure comparability and consistency across studies, reflecting relevant midpoint indicators for environmental performance assessments. The eight environmental impact category indicators identified are::

– Global warming potential (GWP), [kg CO_2-eq.];
– Acidification potential (AP), [kg SO_2-eq.];
– Eutrophication potential (EP), [PO_4^{3-} -eq.];
– Photochemical ozone creation potential (POCP), [kg C_2H_4-eq.],;
– Ozone depletion potential (ODP), [kg CFC^{-11}-eq.];
– Abiotic depletion potential (ADPe) for minerals and metals), [kg Sb-eq.];
– Abiotic depletion potential (ADPf) for fossil resources, [MJ]; and
– Water deprivation potential (WDP), [m^3 e depr.].

2.2.2. Life cycle inventory analysis

Regarding the inventory phase and the related data collection, primary data, directly provided by the Electrical Engineering research team of the University of Palermo which developed the LMA control algorithm within the Sustainable Mobility Center (CNMS) project, were integrated with secondary data from the Ecoinvent database ("Database - ecoinvent," n.d.). The collected primary data are reported in Appendix A and consist of the input powers to the three-phase induction motor expressed as function of the load torque and given rotor speed for the traditional field-oriented control algorithm and the power loss minimization algorithm, respectively (Bruno et al., 2021). In detail, Tables A1 and A2 show the input powers to the three-phase induction motor expressed as a function of the load torque [Nm] and given rotor speed (ω_{ref} = 50–300 [rad/s] with steps of 50 [rad/s]) for the FOC and LMA algorithms, respectively. As can be seen from the comparison between the induction motor input powers in all investigated operating conditions and for both control algorithms that are listed in Appendix Tables A1 and A2 and diagrammed in (Bruno et al., 2021), the LMA algorithm guarantees better performance, recording lower input powers, compared to the traditional control algorithm for any working condition of the three-phase induction motor. It follows that an electric boat that uses the LMA control algorithm will have lower energy consumption and therefore lower environmental impacts, which will be accounted for through the Life Cycle Impact Assessment (LCIA) analysis. Based on these considerations, primary and secondary data were processed to obtain the potential impacts linked to the use phase of the three-phase induction motor operating with both algorithms (traditional and optimized power losses minimization control algorithms). Since the

Table 2
Eco-profiles of each analysed scenario.

Scenario	Description	Eco-profile
1	Electricity produced by the Italian energy mix	1 kWh Electricity, low voltage {IT}| market
2	Electricity produced by the European energy mix	1 kWh Electricity, low voltage {RER}| market
3	Electricity produced by photovoltaic systems	1 kWh Electricity, low voltage {IT}| electricity production, photovoltaic, 3kWp, single-Si panel
4	Electricity produced by thermoelectric power plant powered by fuel oil	1 kWh Electricity, high voltage {IT}| electricity production, oil
5	Electricity produced by diesel-electric generators	1 kWh Electricity production (obtained from the eco-profile of 1 kWh Diesel, burned in fishing vessel {GLO})

primary purpose of the study is to evaluate the potential environmental benefits achievable by optimized electric motor control through the implementation of an LMA algorithm, the analysis focuses exclusively on the motor's operational phase, evaluating the impacts related to electricity consumption. This assumption stems from the condition of substantial equivalence between the life cycle phases excluded from the system boundaries, whether the motor operates with the FOC algorithm or is controlled by the LMA algorithm.

Regarding secondary data, the eco-profiles shown in Table 2 were considered.

Due to the direct lack of the eco-profile for scenario 5 in the environmental used database (Electricity produced by diesel-electric generators), it was necessary to model it through some assumptions. Specifically, an average consumption of a diesel-electric generating set of 0.3 l/kWhe, a Lower Heating Value (LHV) of diesel equal to 11.87 kWh/kg and a diesel density equal to 835 kg/m^3 were considered. Starting from these assumptions and using the eco-profile of diesel burned in fishing vessel (1 kWh Diesel, burned in fishing vessel {GLO}), authors derived the eco-profile for scenario 5.

3. Life cycle environmental impacts assessment: results and discussion

Environmental impacts relating to the absorbed electrical energy by the three-phase induction motor, varying the operating conditions and the used control algorithm, were estimated using the following calculation method: EPD (2018) V1.04 ("Environmental Performance Indicators | EPD International," 2025). By plotting the results of the life cycle impact assessment phase in a three-dimensional Cartesian coordinate system, all impact categories, being a proportional function of the

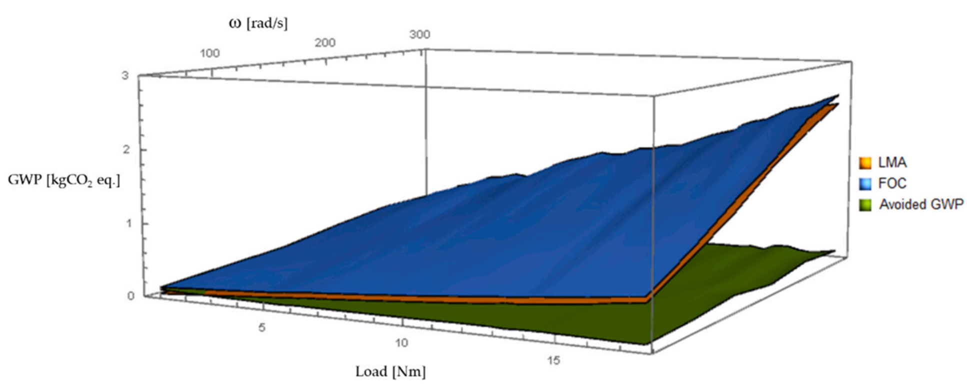

Fig. 3. Comparison between GWP trends as a function of the load torque and rotor speed with the adoption of the traditional FOC (blue surface), the proposed LMA (orange surface), and the avoided GWP (green surface) for Scenario 1.

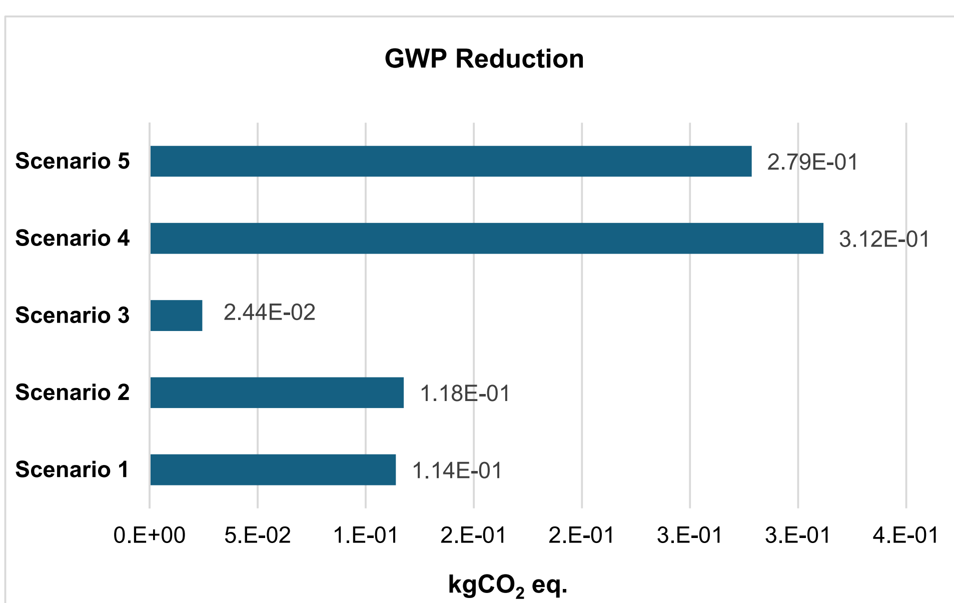

Fig. 4. Variation of GWP reduction as the scenario changes.

Table 3
Percentage reduction of generated impacts (valid for all impact categories) using the LMA algorithm as a function of the load torque and for ω= 50 – 300 (rad/s) with increments of 50 (rad/s). Rotor speed values are expressed in rad/s (1 rad/s = 9.55 rpm).

Percentage reduction of generated impacts by the loss minimization (LMA) algorithm											
***w* = *50* [rad/s]**		***w* = *100* [rad/s]**		***w* = *150* [rad/s]**		***w* = *200* [rad/s]**		***w* = *250* [rad/s]**		***w* = *300* [rad/s]**	
Load [Nm]	**Δ*I* [%]**	**Load [Nm]**	**Δ*I* [%]**	**Load [Nm]**	**Δ*I* [%]**	**Load [Nm]**	**Δ*I* [%]**	**Load [Nm]**	**Δ*I* [%]**	**Load [Nm]**	**Δ*I* [%]**
0.7	73.2 %	0.5	62.6 %	0.4	67.3 %	0.5	26.2 %	0.5	33.2 %	0.5	33.0 %
1.0	68.1 %	0.9	63.8 %	1.0	62.9 %	1.0	24.6 %	1.0	32.7 %	1.0	23.7 %
1.7	57.8 %	1.5	48.2 %	1.4	51.0 %	1.5	24.5 %	1.5	31.9 %	1.5	27.9 %
2.0	54.0 %	1.9	42.3 %	1.8	47.0 %	2.0	25.3 %	2.0	25.5 %	2.0	30.1 %
2.4	49.8 %	2.3	37.8 %	2.2	43.4 %	2.5	19.9 %	2.5	23.1 %	2.5	24.7 %
2.9	45.5 %	2.8	35.5 %	2.6	39.3 %	3.0	23.4 %	3.0	26.9 %	3.0	18.1 %
3.4	40.8 %	3.3	32.2 %	3.1	35.4 %	3.5	20.2 %	3.5	24.9 %	3.5	23.4 %
4.0	37.8 %	3.9	28.5 %	3.8	31.5 %	4.0	18.0 %	4.0	24.0 %	4.0	20.2 %
4.6	32.9 %	4.5	25.5 %	4.5	27.0 %	4.5	17.7 %	4.5	20.6 %	4.5	21.7 %
5.1	30.1 %	5.0	30.3 %	5.0	29.8 %	5.0	10.3 %	5.0	16.4 %	5.0	13.7 %
5.5	28.7 %	5.5	28.3 %	5.4	28.3 %	5.5	9.9 %	5.5	17.7 %	5.5	11.9 %
6.0	29.8 %	6.1	25.2 %	5.8	26.0 %	6.0	12.1 %	6.0	12.3 %	6.0	11.6 %
6.3	27.8 %	6.5	23.7 %	6.3	24.8 %	6.5	9.4 %	6.5	12.8 %	6.5	14.0 %
6.9	27.0 %	6.9	23.0 %	6.8	24.0 %	7.0	9.7 %	7.0	15.7 %	7.0	15.0 %
7.3	25.7 %	7.3	21.1 %	7.3	22.1 %	7.5	11.0 %	7.5	12.5 %	7.5	11.6 %
7.8	24.6 %	7.8	20.3 %	7.7	20.8 %	8.0	6.9 %	8.0	9.7 %	8.0	12.3 %
8.3	23.9 %	8.3	18.7 %	8.2	20.1 %	8.5	10.8 %	8.5	10.4 %	8.5	12.0 %
8.8	22.9 %	8.7	18.6 %	8.6	18.8 %	9.0	4.7 %	9.0	6.8 %	9.0	7.4 %
9.3	22.3 %	9.3	17.5 %	9.2	18.3 %	9.5	5.8 %	9.5	8.3 %	9.5	6.7 %
9.9	21.3 %	9.9	16.3 %	9.7	16.7 %	10.0	4.7 %	10.0	9.4 %	10.0	7.3 %
10.4	20.8 %	10.3	16.3 %	10.3	16.5 %	10.5	2.5 %	10.5	7.9 %	10.5	6.0 %
11.0	20.4 %	10.9	15.3 %	11.0	15.4 %	11.0	2.0 %	11.0	5.5 %	11.0	4.5 %
11.6	20.2 %	11.6	14.7 %	11.5	14.8 %	11.5	4.4 %	11.5	5.1 %	11.5	5.0 %
12.2	19.4 %	12.2	13.4 %	12.0	13.9 %	12.0	4.5 %	12.0	6.2 %	12.0	5.0 %
12.7	18.9 %	12.7	12.8 %	12.4	13.2 %	12.5	4.1 %	12.5	4.1 %	12.5	4.1 %
13.2	16.0 %	13.2	12.6 %	13.0	13.1 %	13.0	4.2 %	13.0	5.3 %	13.0	4.4 %
13.7	17.6 %	13.5	11.8 %	13.4	12.7 %	13.5	2.9 %	13.5	5.2 %	13.5	4.1 %
14.0	17.3 %	14.0	11.4 %	13.6	14.4 %	14.0	4.6 %	14.0	6.9 %	14.0	4.0 %
14.4	17.2 %	14.4	11.9 %	14.0	14.0 %	14.5	4.0 %	14.5	6.6 %	14.5	4.7 %
14.9	15.8 %	14.8	11.6 %	14.6	13.5 %	15.0	3.2 %	15.0	6.6 %	15.0	2.9 %
15.3	15.4 %	15.2	11.4 %	15.0	13.3 %	15.5	2.5 %	15.5	5.1 %	15.5	6.1 %
15.8	14.1 %	15.7	11.3 %	15.5	13.4 %	16.0	3.5 %	16.0	7.0 %	16.0	6.0 %
16.2	13.5 %	16.1	10.7 %	15.9	12.8 %	16.5	4.1 %	16.5	7.3 %	16.5	4.2 %
16.6	12.3 %	16.6	10.7 %	16.4	11.2 %	17.0	1.7 %	17.0	7.5 %	17.0	3.1 %
17.1	12.1 %	17.0	10.3 %	17.0	11.2 %	17.5	0.7 %	17.5	5.6 %	17.5	3.8 %
17.6	11.5 %	17.5	10.1 %	17.5	11.6 %	18.0	4.3 %	18.0	7.7 %	18.0	5.0 %
18.0	11.1 %	18.0	9.7 %	18.0	12.2 %						
18.5	11.3 %	18.4	9.2 %	18.5	13.2 %						
19.0	11.2 %	18.9	9.0 %	19.0	12.8 %						
19.5	11.2 %	19.4	7.6 %	19.4	12.8 %						
		19.9	7.2 %	19.9	13.0 %						
		20.3	7.0 %								

energy absorbed by the motor during its operating phase, show the same trends by varying the motor operating condition. This is a direct consequence of the assumptions made in terms of defining the system boundaries. Only the impacts generated by the operational phase (*i.e.*, energy consumption as the motor operating conditions vary) are assessed and it is assumed that the motor production, maintenance and end-of-life phases are equivalent to the control algorithm variation. It follows that the obtained results can be extended to any impact category; even those do not present in the calculation methodology selected for the study. Therefore, it will be possible to examine the variation of all analysed impact categories by examining one, assumed as representative. In particular, the GWP was selected for its scientific importance and relevance for society and policy committed to counteracting the declared and worrying climate changes (Cusenza et al., 2019; UNFCCC, 2015).

Fig. 3 shows the trends of the GWP impact by varying the load torque and rotor speed for the first analysed scenario (Italian energy mix). Each plotted trend represents the GWP produced by the induction motor controlled by the traditional FOC algorithm (blue trend) and by the LMA algorithm (orange trend). The impact saved by replacing the traditional algorithm with the optimized one is shown by the green surface.

As shown in the graph in Fig. 3, the GWP value increases simultaneously with both the load torque and the rotor speed. Specifically, it can be noted that as rotor speed increases, the environmental impact increases more rapidly as a function of load torque.

Considering the scenario where electricity is generated by Italian energy mix, the average saving in terms of GWP generated using the LMA algorithm compared to traditional FOC algorithm under all induction motor operating conditions is equal to 1.14E-01 kg CO_2-eq. This saving is calculated as the average value over rotor speed of the avoided impacts, averaged over the load torque. As shown in Fig. 4, comparing the different scenarios of electricity generation, it is found that the lowest saving, 2.44E-02 kg CO_2-eq., is obtained when the electrical energy absorbed by the motor is produced by photovoltaic, while the scenarios with the highest GWP reductions are those that present an energy exclusively dependent on fossil fuels such as the thermoelectric power plant powered by fuel oil (3.12E-01 kg CO_2-eq.), and the diesel-electric generators for fishing vessel (2.79E-01 kg CO_2-eq.).

Therefore, the environmental benefits obtainable from the use of the LMA algorithm during the motor operational phase increases with the share of non-renewable energy present in the production mix of the country in which the vessel operates. In percentage terms, the incidence

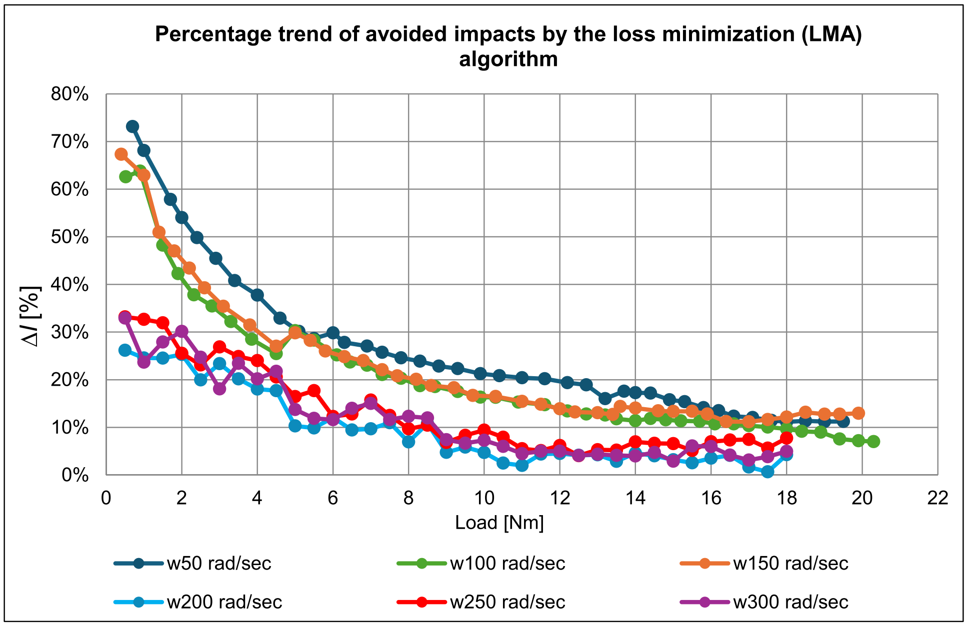

Fig. 5. Trends of the percentage reduction of generated impacts (valid for all impact categories) using the LMA algorithm as a function of the load torque and for ω= 50 – 300 (rad/s) with increments of 50 (rad/s). Rotor speed values are expressed in rad/s (1 rad/s = 9.55 rpm).

of the LMA algorithm compared to the use of the traditional algorithm is around 12 % regardless of the analysed scenario.

Analysing the average saving in terms of generated GWP as a function of the rotor speed, it is possible to state that regardless of the investigated scenario, the highest average saving is obtained at a speed of 150 rad/s, while the lowest average saving is obtained at a speed of

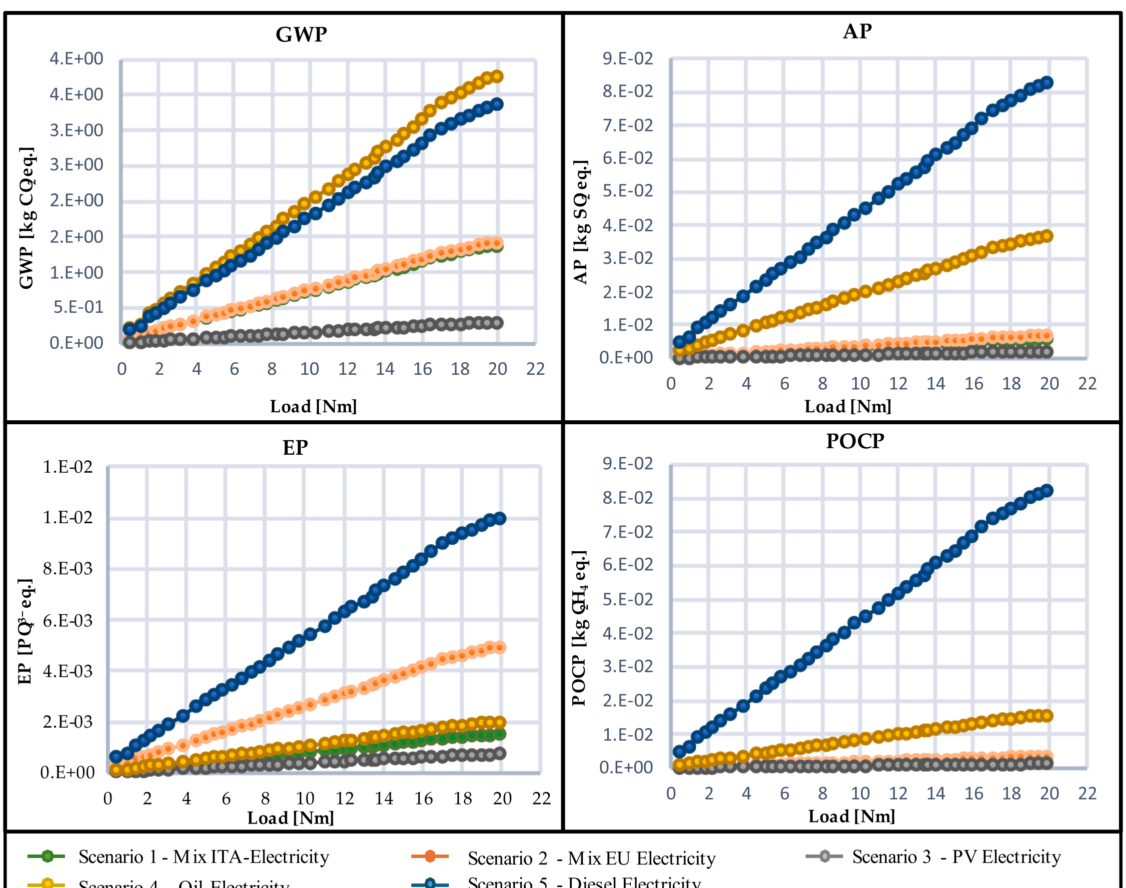

Fig. 6. Comparison of the GWP, AP, EP and POCP trends linked to the three-phase induction electric motor controlled by the LMA algorithm varying the analysed scenario.

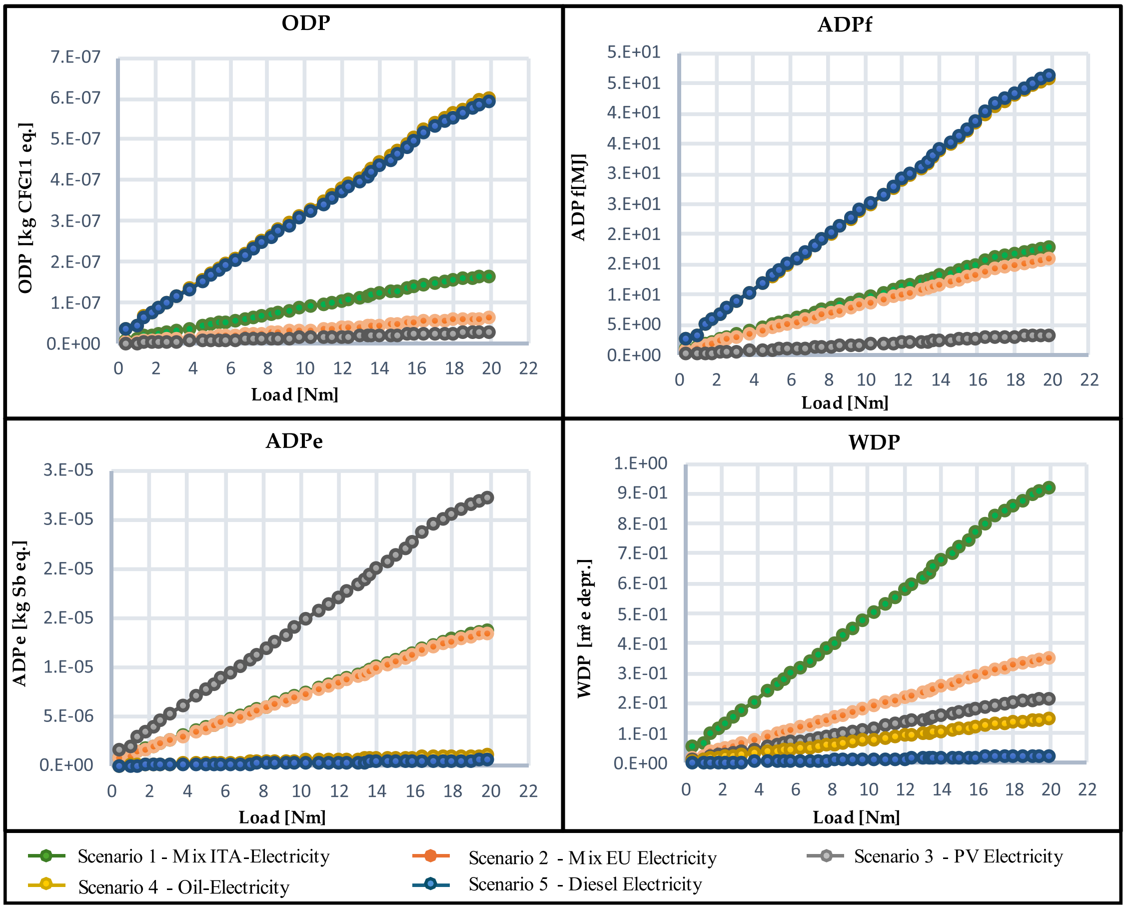

Fig. 7. Comparison of the ODP, ADPf, ADPe and WDP trends linked to the three-phase induction electric motor controlled by the LMA algorithm varying the analysed scenario.

200 rad/s.

3.1. Percentage trend of avoided impacts by the loss minimization (LMA) algorithm

Regardless of the selected impact category, the advantage of adopting the LMA algorithm compared to the FOC algorithm, can also be visualized through the calculation of the avoided impact percentage variation ($\Delta I\%$) by considering Eq. (1):

$$\Delta I\% = \frac{I_{FOC} - I_{LMA}}{I_{FOC}} \cdot 100 \tag{1}$$

where:

I is the generic calculated impact;

I_{FOC} is the generic impact calculated when the three-phase induction motor is controlled using the FOC algorithm; and

I_{LMA} is the generic impact calculated when the three-phase induction motor is controlled using the LMA algorithm.

Table 3 collects the avoided impact percentage variations as a function of the load torque and for each of the 6 analysed rotor speeds. These results are valid for all selected impact categories. Anyway, this analysis is useful to identify the conditions in which the use of the power loss minimizer is more advantageous compared to the FOC.

For a better and more immediate understanding of the operating conditions in which the LMA algorithm allows for minimizing the generated impacts, the results are also plotted in the graph in Fig. 5.

Analysing the graph in Fig. 5, the LMA algorithm allows for obtaining a greater generated impact percentage reduction for low and medium torque loads. In detail, for the rotor speed range from 50 to 150 rad/s, an impact reduction of approximately 60–70 % is obtained for the lowest loads. However, the benefit obtained tends to decrease progressively as the load torque increases and then reduces to values of approximately 10 % for working conditions close to those nominal values. Unlike in the highest rotor speed range (200–300 rad/s), this reduction range is less marked; in this case, the most significant reduction is approximately 30 % at the lowest load torques and then reaches around 5–10 % for the highest load torques. Generally, although its application has a greater impact in operating conditions far from the nominal ones, it can be stated that the algorithm developed in (Bruno et al., 2021) allows to achieve an improved efficiency, and a consequent environmental benefit during the operating phase of the electric motor in any of its operating conditions. In particular, the highest percentage reduction of generated impacts is obtained for the lowest load torques with a reduction that stands at around 30 % and then drops to 15 % for medium torque loads and approximately to 10 % for high torque loads.

3.2. Scenario analysis

In this paragraph, a scenario analysis is performed that aims to show how much and how each impact category is affected by the methods of production of the electrical energy consumed by the motor at varying operating conditions. As highlighted by the results, since 150 rad/s is one of the speeds in which the highest environmental benefit was obtained, the authors decided to conduct this analysis as a function of the load torque and for this rotor speed taken as a reference. In each of the graphs shown in Figs. 6 and 7, for each impact category, the impacts related to the operating phase of the electric motor working with LMA algorithm are compared for each of the five studied scenarios.

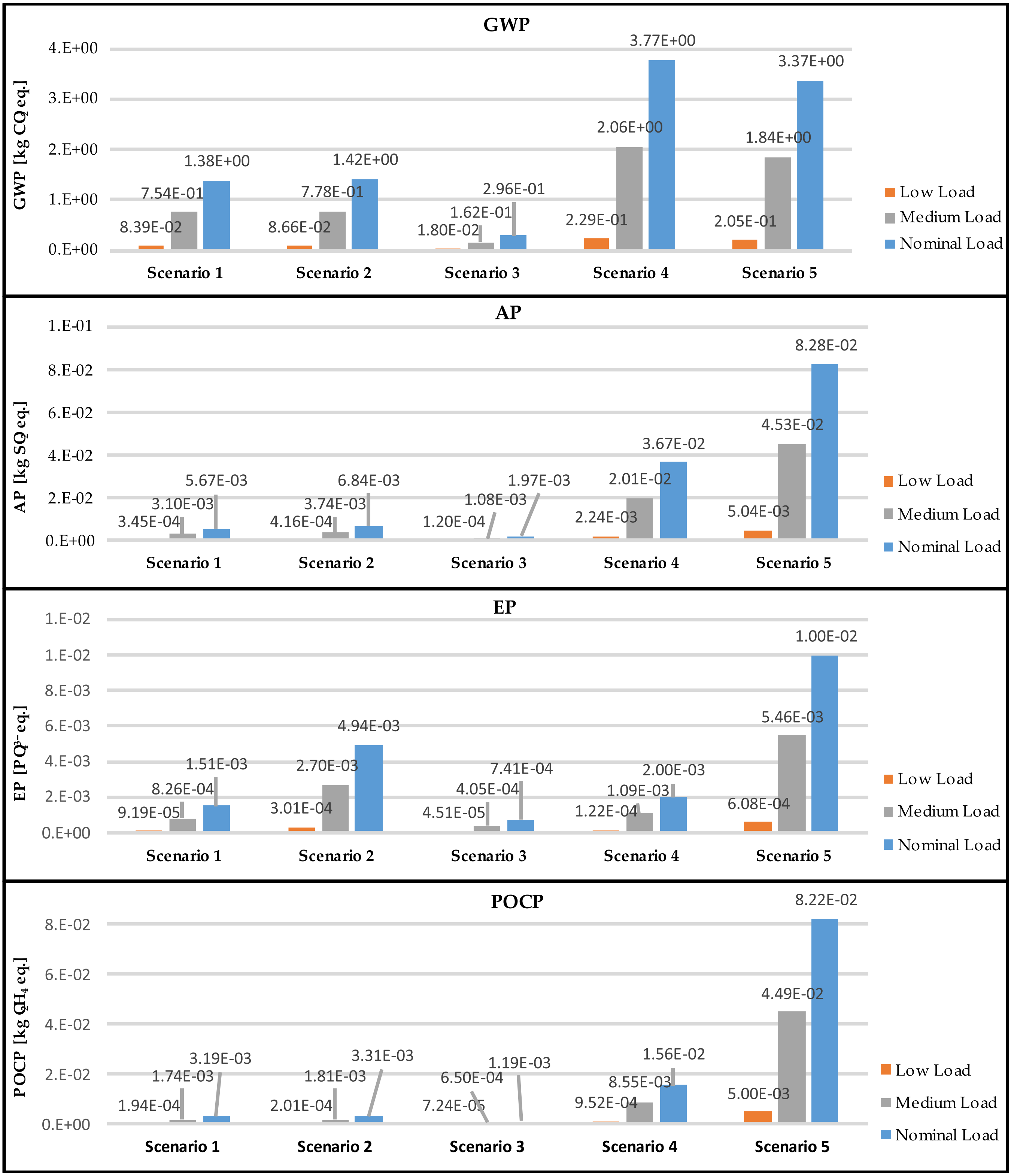

Fig. 8. GWP, AP, EP and POCP impact categories linked to the three-phase induction electric motor controlled by the LMA algorithm for low, medium and nominal load conditions and for each scenario.

Globally, referring to Figs. 6 and 7 it can be said that for almost all the impact investigated categories, except ADPe and WDP, the most environmentally performing scenario is represented by Scenario 3 (electricity produced by photovoltaic), in which the presence of a combustion-free system allows avoiding the emission of those polluting substances that considerably contribute to the formation of the GWP, AP, EP, POCP, ODP, and ADPf indicators. For the same reasons, and the same impact categories, the least environmentally performing scenarios are represented by scenario 4 (electricity from fuel oil) and scenario 5 (electricity from diesel), which, in some cases (GWP, ODP and ADPf),

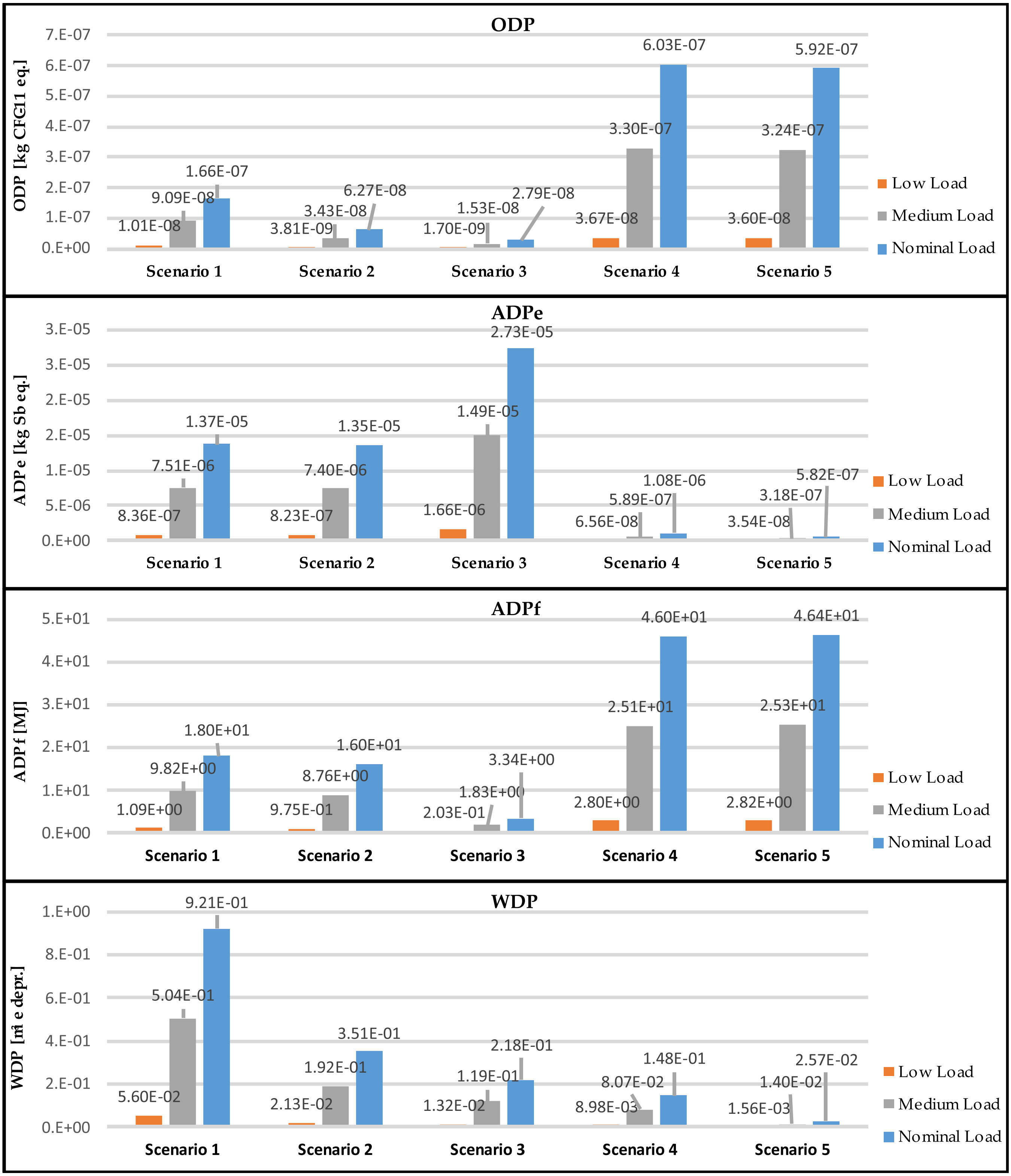

Fig. 9. ODP, ADPe, ADPf and WDP impact categories linked to the three-phase induction electric motor controlled by the LMA algorithm for low, medium and nominal load conditions and for each scenario.

present very close if not overlapping trends. Scenarios 1 (electricity from Mix ITA) and Scenario 2 (electricity from Mix EU) are placed in an intermediate position because, in both cases, within the considered energy mix, there is a significant contribution from renewable sources (hydroelectric, wind and solar sources). A diametrically opposite situation is obtained for the ADPe impact category, in which the least impactful scenarios are Scenarios 4 and 5, while the most impactful one is Scenario 3. The unit of measurement of this index derives from the ratio between the annual global production of a generic resource and the square of its final reserve compared to a reference substance, highlighting how the

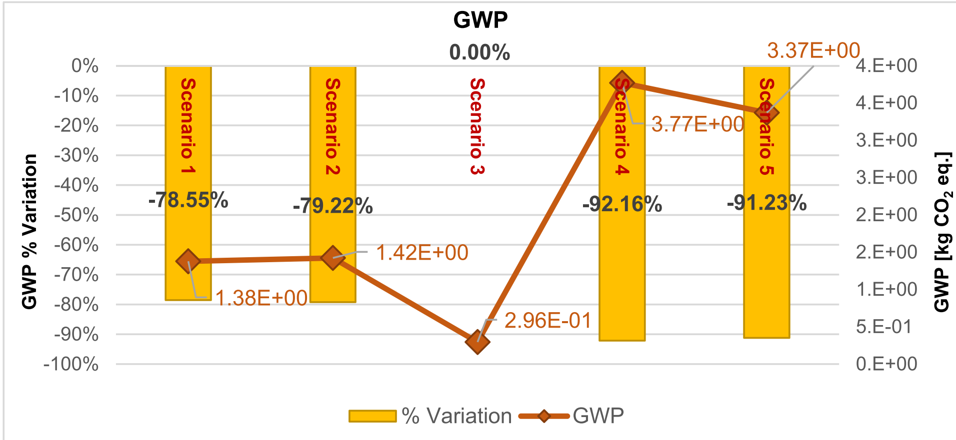

Fig. 10. GWP impact value and percentage variation between scenarios.

materials/resources used in this technology, and in particular silicon, have a significantly higher weight than those used in the other scenarios. About the WPD index, which evaluates the potential deprivation of water for humans or for ecosystems, based on the assumption that if less water remains available per area, it is more likely that another user will be deprived, the most eco-friendly scenario is represented by the Scenario 5 while the worst scenario is represented by Scenario 1 due to a significant percentage of hydroelectric energy within the Italian energy mix.

In absolute terms and to better understand how much and how each impact category is affected by the electricity production methods, Figs. 8 and 9 show the impacts generated by the induction motor operating at 150 rad/s for each scenario. For each scenario, the impacts for low (0.4 Nm), medium (10.3 Nm) and nominal (19.9 Nm) load conditions are plotted.

More in detail, evaluating the percentage change between the scenarios, for the GWP impact category (Fig. 10), the absence of GHG emissions during electricity production in Scenario 3 means that the $kgCO_2$-eq. generated by the motor are 92.16 % lower than in Scenario 4, 91.23 % lower than in Scenario 5, and approximately 79 % lower than in Scenarios 1 and 2.

Referring to the AP, EP and POCP impact categories (Fig. 11), the best scenario (Scenario 3) presents a reduction of the impact between 92 % and 98 % compared to the worst scenario (Scenario 5). Compared to Scenario 4, the variation instead oscillates between 63 % in the case of the EP impact category and approximately 93 % for the other two indicators. Instead, the other scenarios present similar behaviours, with comparable percentage reductions between 60 % and 70 %, except for the EP impact category, which attests a reduction of 85 % for Scenario 2 and 51 % for Scenario 1.

As shown in Fig. 12, for ODP and ADPf impact categories, the worst scenarios, with a completely overlapping trend, are Scenarios 4 and 5. In this case, Scenario 3 presents a maximum reduction of the impact between 92 % and 95 %, a reduction between 81 % and 83 % compared to the scenario based on the Italian energy mix (Scenario 1) and respectively of 55.48 % and 79.15 % compared to the European one (Scenario 2).

The ADPe index results, illustrated in Fig. 13, are different. In this case, the distribution among the scenarios is reversed compared to the previous cases. In particular, Scenario 5 presents a reduction in kg of SO_2-eq. generated of 98 % compared to Scenario 3, of 95 % for Scenarios 1 and 2 and of 46 % compared to Scenario 4.

In the end, completely different results and trends compared to the previous ones can be attributed to the WDP impact category (Fig. 14). In this case, where the impact is linked to the water consumption involved in each scenario, the one with the best environmental performance is represented by Scenario 5, while the worst is represented by Scenario 1. In terms of generated impact reduction, Scenario 5 presents a reduction of 97.21 % compared to Scenario 1, of 92.69 % compared to Scenario 2, and of 88.21 % and 82.61 % for Scenarios 3 and 4, respectively.

4. Multiple linear regression predictive model

Although the application of the LCA methodology represents the optimal solution for the environmental performance assessment of the induction motor operational phase controlled by the LMA algorithm, the computational complexity led the authors to develop a predictive model based on multiple linear regression techniques capable of providing a preliminary estimate of a generic environmental impact category. As anticipated, this model, being easily usable even by an unskilled user without any computational costs, represents a key tool to be used in the planning phase. To obtain reliable results in each motor working condition, the dataset available to the authors has been clustered and divided into two groups: one operating at low load torques and low rotor speed, and the other for intermediate and nominal operating conditions. For each of the two groups, the correlation that best interpolates the impacts obtained from the LCA analysis conducted in the first part of the work has been identified.

The analysis was conducted so that the model predicts the value of the GWP taken as an example transferable to other indicators to create an "early design tool" with a simplified first-use approach that does not aim to replace the traditional LCA but to play an auxiliary role in the very early stages of design.

The developed predictive model is based on the equation expressed in Eq. (2) that explains the relationship between a dependent variable (GWP) and two or more explanatory variables (motor operating conditions: load torque and rotor speed) using a linear combination of the latter. The data used to create the model were obtained from the results of the LCA analysis conducted in paragraph 3 of this study. The model reliability is guaranteed by the robustness of the database previously built by varying the working conditions of the motor controlled by the LMA algorithm.

$$y_i = k + a_1x_1 + a_2x_2 + \ldots + a_nx_n \quad (2)$$

where,

y_i is the i-th independent variable;
x_i is the i-th explanatory variable;
k is the intercept;
a_i is the i-th regression coefficient.

The accuracy estimation of the developed MLR model was conducted through a statistical analysis of the most common error indices. In particular, the Mean Absolute Percentage Error (MAPE), which indicates

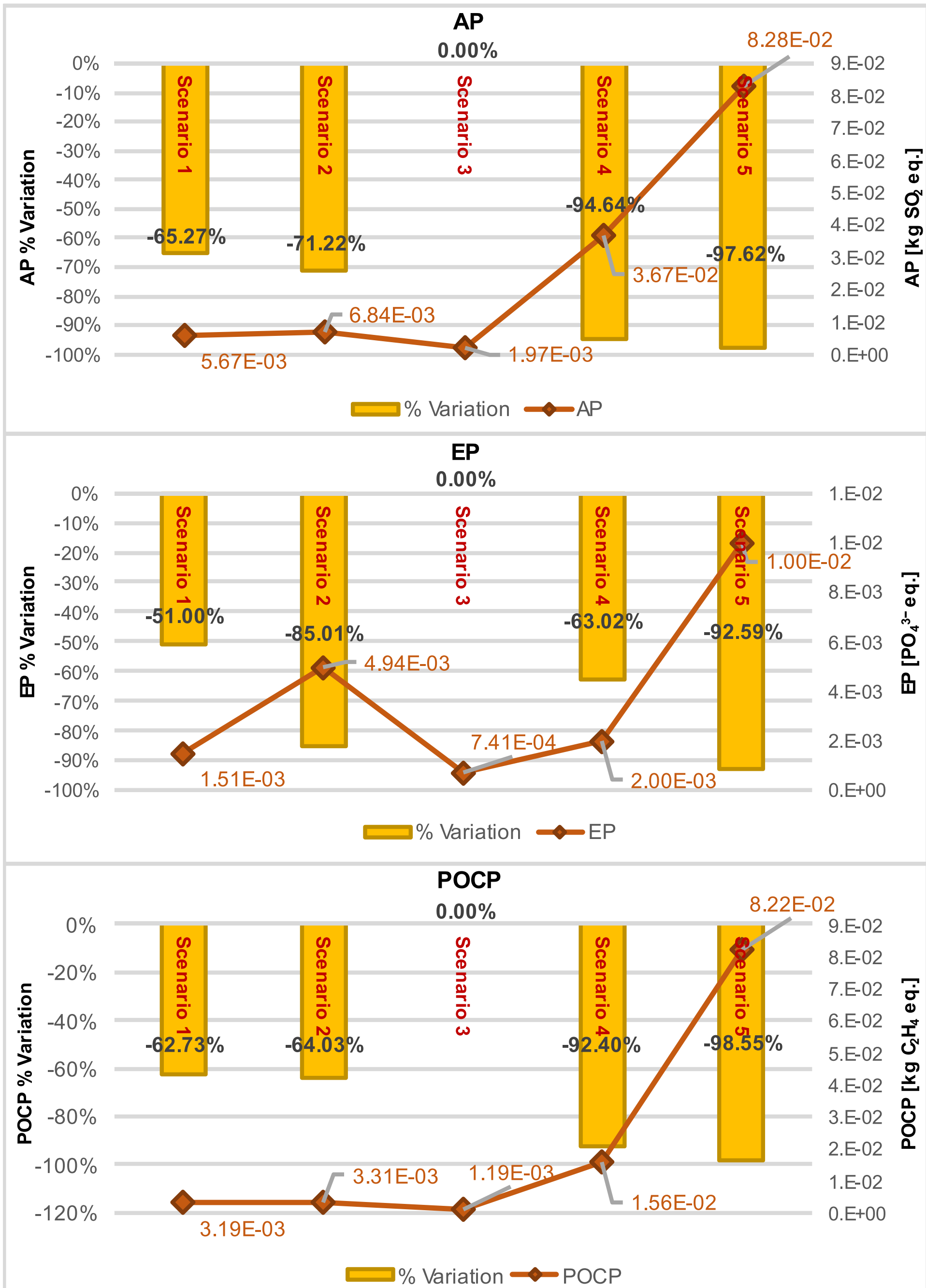

Fig. 11. AP, EP and POCP impact values and percentage variation between scenarios.

the percentage size of the error, and the Root Mean Square Error (RMSE) were calculated. Furthermore, to measure the degree of predictability of the model, the coefficient of determination (R^2) was calculated. The higher the determination coefficient, the more accurate the model is.

4.1. MLR and GWP assessment: results discussion

The form of the equation used to estimate the GWP of the investigated system is represented by Eq. (3):

$$GWP = k + ax + by \tag{3}$$

where,

x is the first explanatory variable (load torque) expressed as [Nm];
y is the second explanatory variable (rotor speed) expressed as [rad/s];
a is the first explanatory coefficient expressed as [kgCO$_2$ eq./Nm];
b is the second explanatory coefficient expressed as [kgCO$_2$ eq. s/rad];
k is the intercept [kgCO$_2$ eq.].

A graphical representation of the equation surface and of the GWP values in all motor working conditions is shown in the Annex (Fig. A1).

The values of the regression coefficients and the intercept obtained are represented in Eq. (4).

$$GWP = -0.646512 + 0.0754569x + 0.00447653y \tag{4}$$

However, from the results analysis, and from a careful visualization of the GWP values distribution with respect to the surface representing the equation, it emerges that, although the coefficient of determination R^2 is equal to 97.5 %, and although this correlation optimally predicts

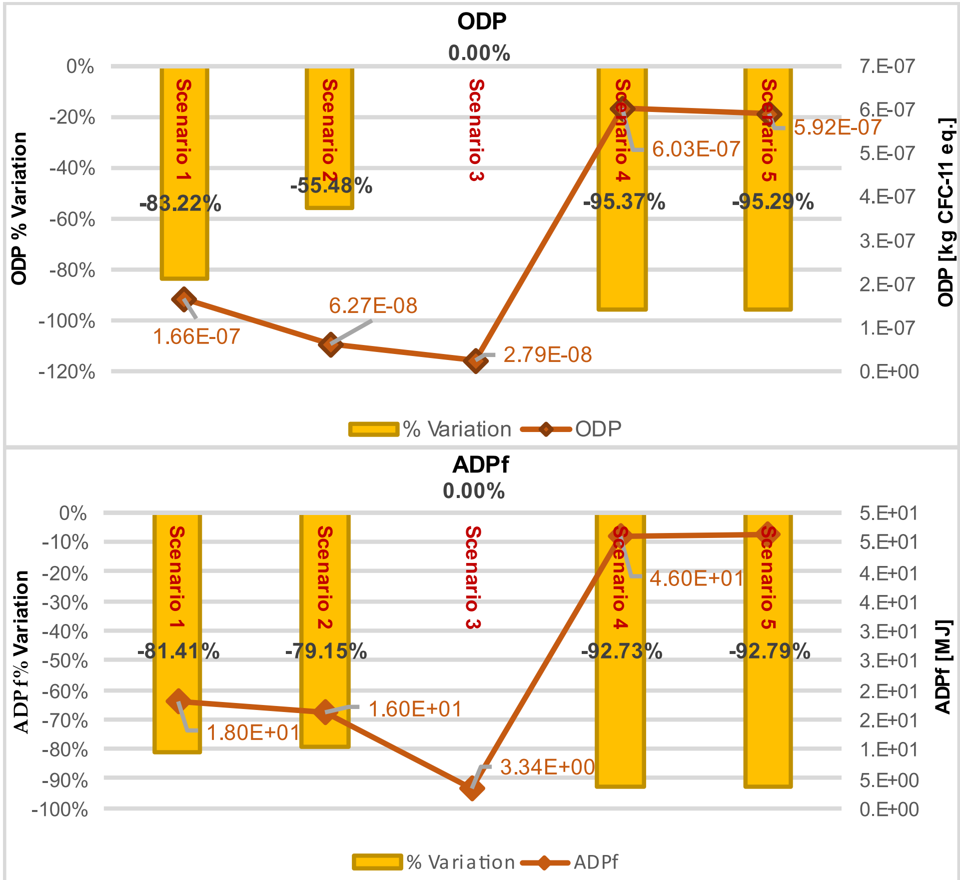

Fig. 12. ODP and ADPf impact values and percentage variation between scenarios.

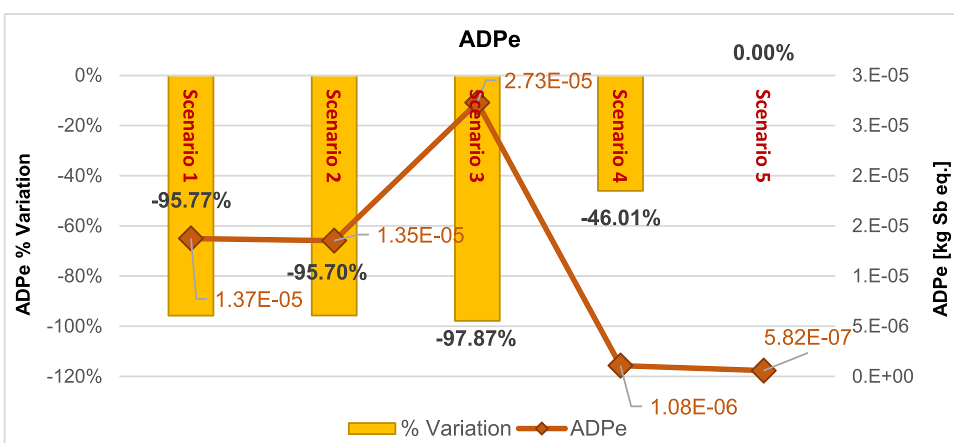

Fig. 13. ADPe impact value and percentage variation between scenarios.

the GWP in almost all motor operating conditions, it is not representative of the lowest load torques at the lowest rotor speeds as the predicted GWP value in these conditions would be negative. Therefore, the authors have clustered the available dataset by dividing it into two groups (A Cluster and B Cluster) and determining a correlation for each of them. The A Cluster is representative of the motor operating points characterized by medium-high load torques and rotor speeds, while the B Cluster by low load torques and low rotor speeds. A graphic representation of the two clusters is reported in the Annex (Fig. A2).

The criteria adopted for the formation of the two clusters are:

$$ACluster = \{\{Load \leq 1 \vee \omega > 150\}; \{1 < Load \leq 4 \vee \omega > 100\};$$

$$\{4 < Load \leq 7.3 \vee \omega > 50\}; \{Load > 7.3 \vee \omega \geq 50\}\}$$

$$BCluster = \{\{Load \leq 1 \vee \omega \leq 150\}; \{1 < Load \leq 4 \vee \omega \leq 100\};$$

$$\{4 < Load \leq 7.3 \vee \omega \leq 50\}\}$$

For both clusters the general equation form (Eq. (3)) is used, and the results are reported in Table 4.

The graphical representations of both cluster correlations are plotted

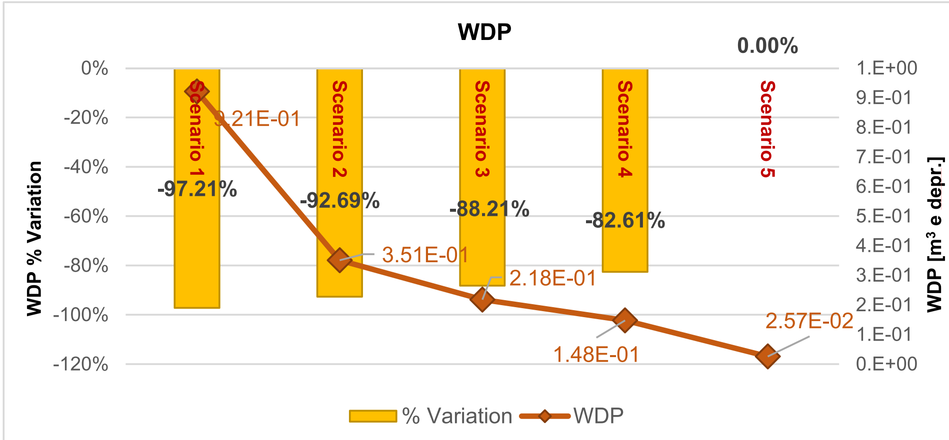

Fig. 14. WDP impact value and percentage variation between scenarios.

Table 4
MLR correlations and determination coefficient for both clusters.

Equation	R^2
$GWP_{ACluster} = -0.894139 + 0.0856784x + 0.00510959y$	98.5 %
$GWP_{BCluster} = -0.038348 + 0.0298421x + 0.00096155y$	97.9 %

in the Annex section (Fig. A3 and Fig. A4).

A first analysis of the results can be done by comparing the dispersion of the points representing the observed and predicted by the MLR model GWP values for both clusters in a 2-dimensional Cartesian coordinate system to the identity line (1:1 line) (Fig. 15).

The closer the points distributed in the graphs of Fig. 15 are placed to the identity line, the more accurate the predictive model is. In addition, to show the reliability of the MLR model developed to calculate the GWP impact category linked to the operational phase of an electric motor controlled by the LMA algorithm in each of its working conditions, the MAPE and RMSE error indices were calculated. Table 5 collects the error indices for both clusters.

The high value of R^2 and the low values of MAPE and RMSE mean that the developed linear regression model can represent a valid alternative able to calculate with a good degree of reliability, and without any computational burdens for the end user, the GWP generated by a three-phase induction electric motor during its operating phase. These simple correlations are suitable to support the decision processes in the preliminary planning phase and significantly accelerate the calculation phase. Finally, a further strength of this work is its replicability. In fact, the applied calculation procedure can be easily replicated and extended to any impact category and nature of the energy source as well as to a wider range of operating conditions and electric motor size. In this way it will be possible to create an "early design tool" that acts as a support in the preliminary design phases by providing a reliable rough estimate linked to any planned design choices.

5. Conclusion

The current study arises from the need to guide the energy transition to a low-carbon economy with clear and relevant information. The transport sector, and in particular naval mobility, characterized by obsolete propulsion systems powered by fossil fuels, is experiencing a strong push towards the development and research of innovative systems, alternative fuels and electrified systems. Electric propulsion systems represent an excellent solution to reduce the environmental impacts of the operative phase of the propulsion system but require a careful assessment of the impacts from a life cycle perspective. To further reduce the environmental pressure of the motor operating phase, optimized control strategies are implemented to improve the efficiency of the electric motor for different load conditions and motor speeds, even far from the nominal operating conditions. Therefore, the authors evaluate the environmental benefits obtainable by using a power losses minimization algorithm in place of a traditional field-oriented control algorithm, starting from the calculation of the environmental impacts of

Table 5
MLR error indices for both clusters.

Dataset	MAPE [%]	RMSE [kg CO_2 eq.]
A Cluster	18.85 %	0.132
B Cluster	11.00 %	0.020

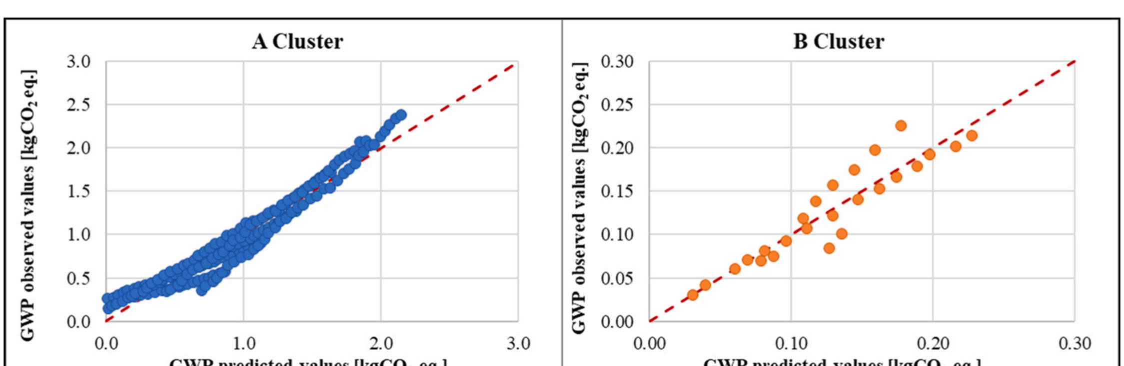

Fig. 15. Comparison of predicted and observed GWP values for both clusters.

a 5.5 kW three-phase induction motor with a double squirrel-cage rotor electric motor during its operational phase under different working conditions. From an analysis of the results, the LMA algorithm guarantees a reduction of the impacts generated in each of the investigated working conditions, with a greater incidence in the motor operating conditions far from the nominal operating conditions. In absolute terms, taking the GWP as an example, the average saving in terms of generated impact using the LMA algorithm compared to traditional FOC algorithm under all induction motor operating conditions is equal to 1.14E-01 kg CO_2-eq. for Scenario 1, 1.18E-01 kg CO_2-eq. for Scenario 2, 2.44E-02 kg CO_2-eq for Scenario 3, 3.12E-01 kg CO_2-eq for Scenario 4 and 2.79E-01 kg CO_2-eq for Scenario 5, demonstrating that the obtainable benefit increases with the share of non-renewable energy present in the energy production mix.

Instead, analysing the percentage variation in each motor operating condition, the widest margin of improvement is obtained for low rotor speeds (between 50 and 150 rad/s) and medium-low load torques with reduction peaks close to 70 %. In general, it can be stated that the highest percentage reduction of generated impacts is obtained for the lowest load torques with a reduction that stands at around 30 % and then drops to 15 % for medium torque loads and approximately to 10 % for high torque loads. These percentage variations are valid for any impact category since only the operating phase of the motor is analysed; it is assumed that the motor production, maintenance and end-of-life phases are equivalent for both algorithms. Furthermore, a scenario analysis aimed at assessing the sustainability of marine electric propulsion systems as a function of the energy carrier used for upstream electricity generation has been performed. The analysis showed that improving the share of renewable energy in electricity improves the environmental performance of the electric motor. In fact, from an environmental point of view, the best performing scenario is the one characterized by electricity entirely produced from renewable sources, in which the presence of a combustion-free system allows avoiding the emission of those polluting substances that considerably contribute to the formation of the GWP, AP, EP, POCP, ODP, and ADPf indicators. Conversely, the least performing scenarios are those characterized by an energy carrier based exclusively on fossil fuels. The same cannot be said for the ADPe and WDP indicators. For these impact categories, the best performing scenarios are those based on electricity consumption from fossil fuels, while the least performing scenarios are respectively the scenario based on photovoltaic energy for the ADPe impact category, and the scenario characterised by a higher share of hydroelectric energy within the production mix for the WDP impact category. This inversion is due respectively to the presence of silicon in photovoltaic panels and a high depletion of water resources in hydroelectric power plants.

In conclusion, the carried-out analyses offer encouraging insights into the usefulness of optimized control systems and indications on the optimal operating conditions to maximize environmental benefits or those on which to focus future research efforts. The obtained results could represent a useful data set and a starting point to evaluate the environmental benefits in operational phase characterised by defined navigation times, rotor speed and resisting torque.

Finally, to overcome the well-known problem of computational complexity that lies behind a complete life cycle assessment analysis, and therefore quickly expand the range of operating conditions analysed, the authors proposed two simple mathematical equations capable of predicting the GWP of the induction electric motor during its operational phase and when the operating conditions vary. The first equation is representative of the motor working conditions characterized by medium-high load torques and rotor speeds (A Cluster), the second by low load torques and low rotor speeds (B Cluster). These correlations, obtained through a linear regression of the data from the performed LCA analysis, present a high degree of reliability and predictability demonstrated by the high value of the determination coefficient and by the values of two of the most common error indices (MAPE and RMSE). In particular, the determination coefficient reaches the values of 98.5 % for A Cluster and 97.9 % for B Cluster respectively. As regards the calculated error indices, the A Cluster correlation obtains a MAPE of 18.85 % and a RMSE of 0.132 020 kg CO_2 eq., while the B Cluster correlation presents a MAPE of 11 % and a RMSE of 0.020 kg CO_2 eq. Therefore, the main strength of the predictive model developed in this work lies in its simplicity of use, since its application does not require any complex calculation tool but consists in solving a linear equation which is able to determine the environmental impacts linked to the motor operative phase. These features make the developed MLR model suitable for use even by a non-expert user, speeding up the environmental impacts estimation. Despite everything, this early design tool is not intended to replace the life cycle assessment but represents a simple and rapid alternative to support the decision-making process in the preliminary planning phase and to have an overall view of the impacts obtainable by varying the operating conditions of the motor. To conclude, the performed approach is generalizable and extendable to any impact category, electric motor size and type of powertrains system simply by changing the input dataset.

CRediT authorship contribution statement

D'Amico Antonino: Writing – review & editing, Writing – original draft, Visualization, Validation, Methodology, Investigation, Formal analysis, Data curation, Conceptualization. **Sonia Longo:** Writing – review & editing, Validation, Supervision, Resources, Conceptualization. **Rosario Miceli:** Writing – review & editing, Supervision, Project administration. **Maurizio Cellura:** Writing – review & editing, Supervision, Resources, Project administration. **Massimo Caruso:** Writing – review & editing, Writing – original draft, Resources.

Declaration of Competing Interest

The authors declare that they have no Known competing financial interests or personal relationship that could have appeared to influence the work reported in this article

Acknowledgement

This research has been partially supported by the European Union - NextGenerationEU - National Sustainable Mobility Center CN00000023, Italian Ministry of University and Research Decree n. 1033— 17/06/2022, Spoke 2, Spoke 3, and Spoke 12, CUP B73C22000760001.

Appendix A

Tables A1 and A2 list all the collected primary data. In detail, Table A1 reports the input power values to the induction motor obtained by varying the load torque and the rotor speed when the traditional FOC control algorithm is used. Table A2 instead shows the input power values when the LMA power loss minimization algorithm controls the induction motor.

Table A1
Input powers to the three-phase induction motor expressed as function of the load torque with the adoption of the traditional FOC algorithm for ω= 50 – 300 (rad/s) with increments of 50 (rad/s) (Bruno et al., 2021)

Input power to the three-phase induction motor controlled by the traditional field-oriented control (FOC) algorithm											
w = 50 [rad/sec]		*w = 100 [rad/sec]*		*w = 150 [rad/sec]*		*w = 200 [rad/sec]*		*w = 250 [rad/sec]*		*w = 300 [rad/sec]*	
Load [Nm]	*Input Power [kW]*	*Load [Nm]*	*Input Power [kW]*	*Load [Nm]*	*Input Power [kW]*	*Load [Nm]*	*Input Power [kW]*	*Load [Nm]*	*Input Power [kW]*	*Load [Nm]*	*Input Power [kW]*
0.7	0.333	0.5	0.514	0.4	0.685	0.5	1.058	0.5	1.365	0.5	1.411
1.0	0.353	0.9	0.554	1.0	0.730	1.0	1.148	1.0	1.470	1.0	1.420
1.7	0.384	1.5	0.613	1.4	0.829	1.5	1.236	1.5	1.625	1.5	1.694
2.0	0.412	1.9	0.640	1.8	0.889	2.0	1.384	2.0	1.677	2.0	1.921
2.4	0.433	2.3	0.674	2.2	0.959	2.5	1.459	2.5	1.867	2.5	2.008
2.9	0.455	2.8	0.723	2.6	1.026	3.0	1.660	3.0	2.158	3.0	2.108
3.4	0.482	3.3	0.779	3.1	1.110	3.5	1.766	3.5	2.215	3.5	2.407
4.0	0.523	3.9	0.842	3.8	1.204	4.0	1.881	4.0	2.352	4.0	2.464
4.6	0.557	4.5	0.920	4.5	1.317	4.5	1.978	4.5	2.455	4.5	2.630
5.1	0.585	5.0	1.061	5.0	1.496	5.0	1.924	5.0	2.463	5.0	2.565
5.5	0.620	5.5	1.126	5.4	1.564	5.5	1.989	5.5	2.599	5.5	2.652
6.0	0.682	6.1	1.179	5.8	1.625	6.0	2.165	6.0	2.664	6.0	2.873
6.3	0.710	6.5	1.229	6.3	1.703	6.5	2.238	6.5	2.861	6.5	3.161
6.9	0.738	6.9	1.296	6.8	1.787	7.0	2.364	7.0	3.060	7.0	3.381
7.3	0.771	7.3	1.326	7.3	1.864	7.5	2.532	7.5	3.147	7.5	3.496
7.8	0.804	7.8	1.385	7.7	1.940	8.0	2.569	8.0	3.276	8.0	3.635
8.3	0.841	8.3	1.435	8.2	2.022	8.5	2.734	8.5	3.468	8.5	3.818
8.8	0.880	8.7	1.510	8.6	2.110	9.0	2.767	9.0	3.441	9.0	3.777
9.3	0.923	9.3	1.567	9.2	2.208	9.5	2.878	9.5	3.638	9.5	3.831
9.9	0.966	9.9	1.631	9.7	2.299	10.0	3.009	10.0	3.732	10.0	4.076
10.4	1.013	10.3	1.712	10.3	2.409	10.5	3.091	10.5	3.878	10.5	4.115
11.0	1.062	10.9	1.786	11.0	2.513	11.0	3.152	11.0	3.937	11.0	4.267
11.6	1.120	11.6	1.860	11.5	2.615	11.5	3.297	11.5	4.046	11.5	4.321
12.2	1.169	12.2	1.928	12.0	2.695	12.0	3.452	12.0	4.248	12.0	4.558
12.7	1.222	12.7	1.992	12.4	2.768	12.5	3.556	12.5	4.340	12.5	4.770
13.2	1.264	13.2	2.053	13.0	2.854	13.0	3.563	13.0	4.495	13.0	4.927
13.7	1.301	13.5	2.097	13.4	2.921	13.5	3.713	13.5	4.645	13.5	5.077
14.0	1.344	14.0	2.159	13.6	3.072	14.0	3.908	14.0	4.831	14.0	5.314
14.4	1.387	14.4	2.226	14.0	3.162	14.5	3.980	14.5	4.963	14.5	5.483
14.9	1.426	14.8	2.288	14.6	3.241	15.0	4.086	15.0	5.163	15.0	5.573
15.3	1.475	15.2	2.341	15.0	3.329	15.5	4.176	15.5	5.236	15.5	5.789
15.8	1.515	15.7	2.415	15.5	3.448	16.0	4.318	16.0	5.462	16.0	6.062
16.2	1.563	16.1	2.472	15.9	3.534	16.5	4.470	16.5	5.585	16.5	6.130
16.6	1.615	16.6	2.543	16.4	3.611	17.0	4.472	17.0	5.684	17.0	6.248
17.1	1.665	17.0	2.611	17.0	3.732	17.5	4.578	17.5	5.846	17.5	6.487
17.6	1.719	17.5	2.684	17.5	3.827	18.0	4.808	18.0	6.021	18.0	6.697
18.0	1.767	18.0	2.759	18.0	3.930						
18.5	1.824	18.4	2.832	18.5	4.048						
19.0	1.873	18.9	2.906	19.0	4.113						
19.5	1.931	19.4	2.964	19.4	4.177						
20.0	NaN	19.9	3.043	19.9	4.229						
20.4	NaN	20.3	3.124								

Table A2
Input powers to the three-phase induction motor expressed as function of the load torque with the adoption of the loss minimization LMA algorithm for ω= 50 – 300 (rad/s) with increments of 50 (rad/s) (Bruno et al., 2021)

Input power to the three-phase induction motor controlled by the loss minimization (LMA) algorithm											
w = 50 [rad/sec]		*w = 100 [rad/sec]*		*w = 150 [rad/sec]*		*w = 200 [rad/sec]*		*w = 250 [rad/sec]*		*w = 300 [rad/sec]*	
Load [Nm]	*Input Power [kW]*	*Load [Nm]*	*Input Power [kW]*	*Load [Nm]*	*Input Power [kW]*	*Load [Nm]*	*Input Power [kW]*	*Load [Nm]*	*Input Power [kW]*	*Load [Nm]*	*Input Power [kW]*
0.7	0.089	0.5	0.192	0.4	0.224	0.5	0.781	0.5	0.912	0.5	0.946
1.0	0.112	0.9	0.201	1.0	0.271	1.0	0.866	1.0	0.990	1.0	1.084
1.7	0.162	1.5	0.317	1.4	0.407	1.5	0.933	1.5	1.106	1.5	1.221
2.0	0.189	1.9	0.369	1.8	0.471	2.0	1.034	2.0	1.249	2.0	1.342
2.4	0.217	2.3	0.419	2.2	0.542	2.5	1.168	2.5	1.436	2.5	1.512
2.9	0.248	2.8	0.466	2.6	0.623	3.0	1.272	3.0	1.578	3.0	1.727
3.4	0.286	3.3	0.528	3.1	0.717	3.5	1.410	3.5	1.664	3.5	1.843
4.0	0.326	3.9	0.602	3.8	0.825	4.0	1.542	4.0	1.787	4.0	1.967
4.6	0.373	4.5	0.686	4.5	0.961	4.5	1.628	4.5	1.950	4.5	2.058
5.1	0.408	5.0	0.740	5.0	1.050	5.0	1.726	5.0	2.058	5.0	2.213
5.5	0.442	5.5	0.807	5.4	1.122	5.5	1.793	5.5	2.139	5.5	2.337
6.0	0.478	6.1	0.882	5.8	1.202	6.0	1.904	6.0	2.337	6.0	2.540

(continued on next page)

Table A2 (*continued*)

Input power to the three-phase induction motor controlled by the loss minimization (LMA) algorithm											
w = 50 [rad/sec]		***w = 100 [rad/sec]***		***w = 150 [rad/sec]***		***w = 200 [rad/sec]***		***w = 250 [rad/sec]***		***w = 300 [rad/sec]***	
Load	***Input Power***	***Load***	***Input Power***	***Load***	***Input Power***	***Load***	***Input Power***	***Load***	***Input Power***	***Load***	***Input Power***
[Nm]	***[kW]***	***[Nm]***	***[kW]***	***[Nm]***	***[kW]***	***[Nm]***	***[kW]***	***[Nm]***	***[kW]***	***[Nm]***	***[kW]***
6.3	0.513	6.5	0.938	6.3	1.280	6.5	2.027	6.5	2.495	6.5	2.719
6.9	0.539	6.9	0.997	6.8	1.358	7.0	2.135	7.0	2.579	7.0	2.873
7.3	0.572	7.3	1.046	7.3	1.452	7.5	2.254	7.5	2.754	7.5	3.089
7.8	0.606	7.8	1.104	7.7	1.536	8.0	2.391	8.0	2.959	8.0	3.188
8.3	0.640	8.3	1.166	8.2	1.616	8.5	2.438	8.5	3.106	8.5	3.361
8.8	0.679	8.7	1.229	8.6	1.714	9.0	2.636	9.0	3.206	9.0	3.497
9.3	0.717	9.3	1.292	9.2	1.804	9.5	2.710	9.5	3.336	9.5	3.576
9.9	0.761	9.9	1.365	9.7	1.915	10.0	2.867	10.0	3.381	10.0	3.780
10.4	0.802	10.3	1.433	10.3	2.012	10.5	3.014	10.5	3.571	10.5	3.868
11.0	0.845	10.9	1.513	11.0	2.125	11.0	3.089	11.0	3.720	11.0	4.076
11.6	0.893	11.6	1.586	11.5	2.227	11.5	3.153	11.5	3.839	11.5	4.106
12.2	0.943	12.2	1.669	12.0	2.321	12.0	3.297	12.0	3.986	12.0	4.331
12.7	0.990	12.7	1.737	12.4	2.402	12.5	3.409	12.5	4.164	12.5	4.576
13.2	1.061	13.2	1.795	13.0	2.481	13.0	3.412	13.0	4.257	13.0	4.712
13.7	1.072	13.5	1.850	13.4	2.550	13.5	3.607	13.5	4.403	13.5	4.869
14.0	1.112	14.0	1.913	13.6	2.630	14.0	3.729	14.0	4.496	14.0	5.103
14.4	1.149	14.4	1.962	14.0	2.718	14.5	3.820	14.5	4.634	14.5	5.225
14.9	1.201	14.8	2.023	14.6	2.805	15.0	3.956	15.0	4.824	15.0	5.412
15.3	1.248	15.2	2.075	15.0	2.885	15.5	4.070	15.5	4.967	15.5	5.437
15.8	1.301	15.7	2.143	15.5	2.987	16.0	4.166	16.0	5.082	16.0	5.700
16.2	1.352	16.1	2.207	15.9	3.082	16.5	4.286	16.5	5.176	16.5	5.874
16.6	1.416	16.6	2.270	16.4	3.206	17.0	4.397	17.0	5.260	17.0	6.053
17.1	1.464	17.0	2.341	17.0	3.315	17.5	4.548	17.5	5.516	17.5	6.238
17.6	1.522	17.5	2.414	17.5	3.382	18.0	4.603	18.0	5.555	18.0	6.365
18.0	1.570	18.0	2.492	18.0	3.452						
18.5	1.617	18.4	2.572	18.5	3.515						
19.0	1.663	18.9	2.645	19.0	3.588						
19.5	1.714	19.4	2.740	19.4	3.644						
20.0	1.764	19.9	2.824	19.9	3.681						
20.4	1.806	20.3	2.905								

The Fig. A1 shows a graphical representation of the equation surface (Eq. (4)) and of the GWP values in all motor working conditions (black points). The x-axis shows the load torque [Nm], the y-axis shows the rotor speed [rad/s] and the z-axis shows the GWP [$kgCO_2$ eq.].

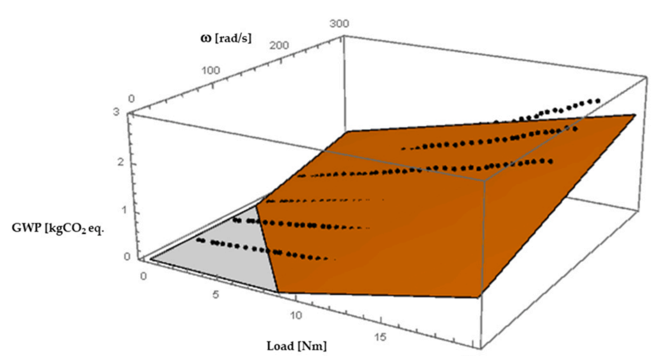

Figure A1. Scatter plot and regression plan for the GWP impact category

Figure A2 plots the working conditions divided between the two clusters identified in the Section 4.1.

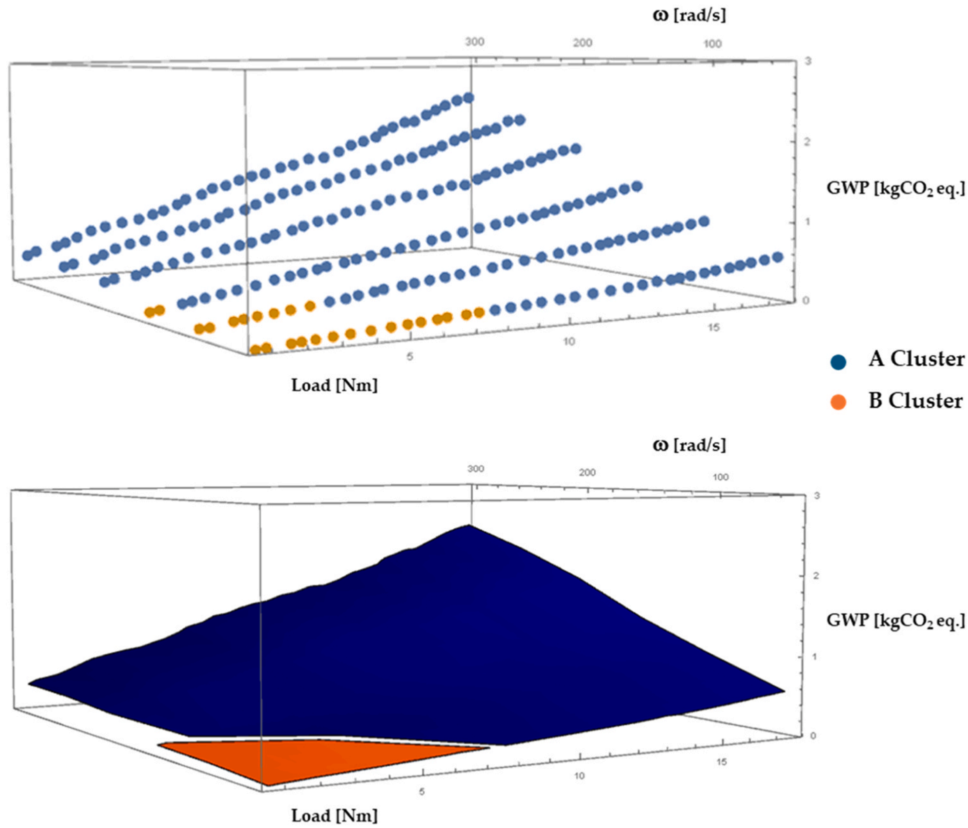

Figure A2. Scatter 3D plot of the A Cluster and B Cluster

Figure A3 and A4 plot the correlations of A and B Clusters.

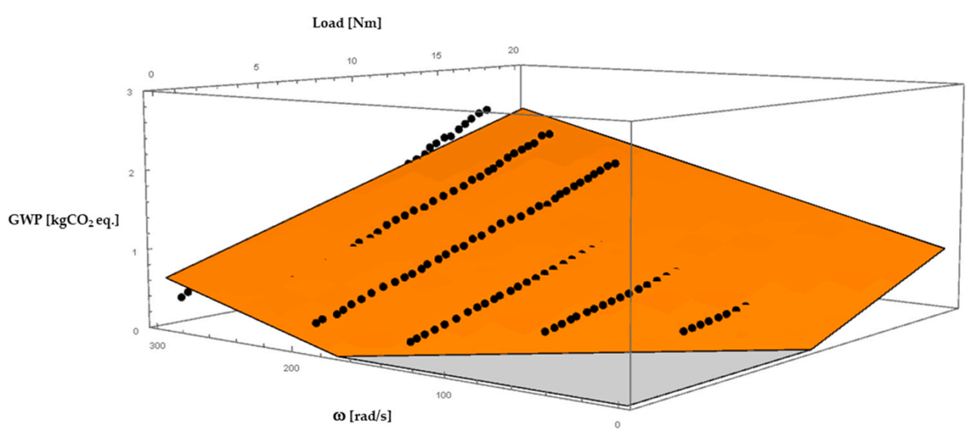

Figure A3. Scatter plot and regression plan for the GWP impact category for the A Cluster

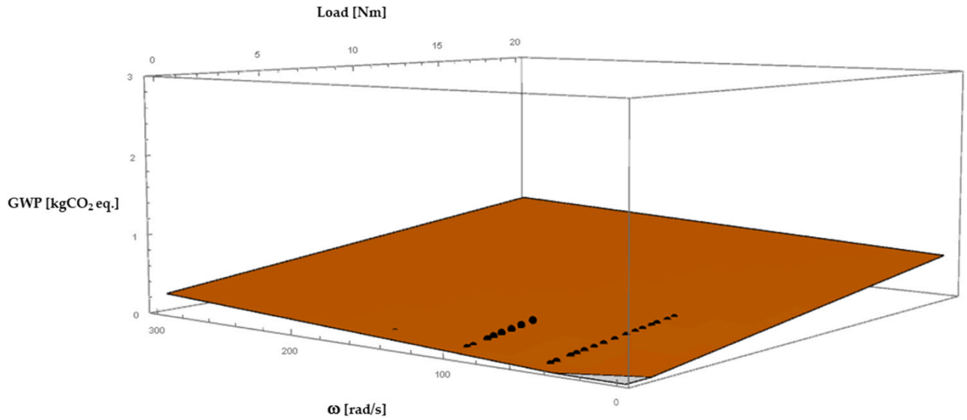

Figure A4. Scatter plot and regression plan for the GWP impact category for the B Cluster

Data availability

Data will be made available on request.

References

Ammar, N.R., Seddiek, I.S., 2021. Evaluation of the environmental and economic impacts of electric propulsion systems onboard ships: case study passenger vessel. Environ. Sci. Pollut. Res. 28, 37851–37866.

Aydinalp-Koksal, M., Ugursal, V.I., 2008. Comparison of neural network, conditional demand analysis, and engineering approaches for modeling end-use energy consumption in the residential sector. Appl. Energy 85, 271–296. https://doi.org/10.1016/j.apenergy.2006.09.012.

Bach, H., Bergek, A., Bjørgum, Ø., Hansen, T., Kenzhegaliyeva, A., Steen, M., 2020. Implementing maritime battery-electric and hydrogen solutions: a technological innovation systems analysis. Transp. Res. Part D. Transp. Environ. 87, 102492.

Blanco-Davis, E., Zhou, P., 2014. LCA as a tool to aid in the selection of retrofitting alternatives. Ocean Eng. 77, 33–41.

Bouman, E.A., Lindstad, E., Rialland, A.I., Strømman, A.H., 2017. State-of-the-art technologies, measures, and potential for reducing GHG emissions from shipping–A review. Transp. Res. Part D. Transp. Environ. 52, 408–421.

Bruno, A., Caruso, M., Di Tommaso, A.O., Miceli, R., Nevoloso, C., Viola, F., 2021. Simple and flexible power loss minimizer with low-cost MCU implementation for high-efficiency three-phase induction motor drives. IEEE Trans. Ind. Appl. 57, 1472–1481.

Ciulla, G., D'Amico, A., 2019. Building energy performance forecasting: a multiple linear regression approach. Appl. Energy 253, 113500. https://doi.org/10.1016/J.APENERGY.2019.113500.

Ciulla, G., Lo Brano, V., D'Amico, A., 2016. Modelling relationship among energy demand, climate and office building features: A cluster analysis at European level. Appl. Energy 183, 1021–1034. https://doi.org/10.1016/j.apenergy.2016.09.046.

Cusenza, M.A., Guarino, F., Longo, S., Mistretta, M., Cellura, M., 2019. Reuse of electric vehicle batteries in buildings: an integrated load match analysis and life cycle assessment approach. Energy Build. 186, 339–354.

D'Amico, A., Ciulla, G., Panno, D., Ferrari, S., 2019. Building energy demand assessment through heating degree days: The importance of a climatic dataset. Appl. Energy 242, 1285–1306. https://doi.org/10.1016/J.APENERGY.2019.03.167.

Database - ecoinvent [WWW Document], n.d. URL ⟨https://ecoinvent.org/database/⟩ (accessed 1.21.25).

Dedes, E.K., Hudson, D.A., Turnock, S.R., 2012. Assessing the potential of hybrid energy technology to reduce exhaust emissions from global shipping. Energy Policy 40, 204–218.

DNV, G.L., 2019. Assessment of selected alternative fuels and technologies in shipping. DNV GL.

Environmental Performance Indicators | EPD International [WWW Document], n.d. URL ⟨https://www.environdec.com/services/environmental-performance-indicators/gpi-5/indicators-of-environmental-impact⟩ (accessed 12.12.25).

Gagatsi, E., Estrup, T., Halatsis, A., 2016. Exploring the potentials of electrical waterborne transport in Europe: the E-ferry concept. Transp. Res. Procedia 14, 1571–1580.

Gu, Y., Wallace, S.W., Wang, X., 2019. Can an Emission Trading Scheme really reduce CO2 emissions in the short term? Evidence from a maritime fleet composition and deployment model. Transp. Res. Part D. Transp. Environ. 74, 318–338.

Hansen, K.N.J., Steinshamn, H., Hansen, S., Koesling, M., Dalgaard, T., Hansen, B.G., 2025. Comparing different statistical models for predicting greenhouse gas emissions, energy-, and nitrogen intensity. Comput. Electron. Agric. 234, 110209.

Hemez, C., Chiu, J., Ryan, E.C., Sun, J., Dubrow, R., Pascucilla, M., 2020. Environmental and health impacts of electric service vessels in the recreational boating industry. Water Pract. \ Technol. 15, 781–796.

IMO, 2024. International Maritime Organization [WWW Document]. URL ⟨https://www.imo.org/⟩ (accessed 6.10.24).

International EPD System, 2025. General Programme Instructions for the International EPD System (Version 5.0.1).

International Organization for Standardization (ISO), 2020. ISO 14040:2006/Amd 1: 2020 Environmental management - Life cycle assessment - Principles And Framework.

Jeong, B., Jang, H., Lee, W., Park, C., Ha, S., Cho, N.-K., others, 2022. Is electric battery propulsion for ships truly the lifecycle energy solution for marine environmental protection as a whole? J. Clean. Prod. 355, 131756.

Jianyun, Z., Li, C., Lijuan, X., Bin, W., 2019. Bi-objective optimal design of plug-in hybrid electric propulsion system for ships. Energy 177, 247–261.

Kim, S., Jeon, H., 2022. Comparative analysis on AC and DC distribution systems for electric propulsion ship. J. Mar. Sci. Eng. 10, 559.

Kim, S., Jeon, H., Park, C., Kim, J., 2022. Lifecycle environmental benefits with a hybrid electric propulsion system using a control algorithm for fishing boats in Korea. J. Mar. Sci. Eng. 10, 1202.

Lu, Y., Shao, M., Zheng, C., Ji, H., Gao, X., Wang, Q., 2020. Air pollutant emissions from fossil fuel consumption in China: Current status and future predictions. Atmos. Environ. 231, 117536.

Monteiro, A., Russo, M., Gama, C., Borrego, C., 2018. How important are maritime emissions for the air quality: At European and national scale. Environ. Pollut. 242, 565–575.

Ng, W.L., Azmi, A.M., Dahlan, N.Y., Woon, K.S., 2024. Predicting life cycle carbon emission of green office buildings via an integrated LCA-MLR framework. Energy Build. 316, 114345.

Perčić, M., Frković, L., Pukšec, T., Ćosić, B., Li, O.L., Vladimir, N., 2022. Life-cycle assessment and life-cycle cost assessment of power batteries for all-electric vessels for short-sea navigation. Energy 251, 123895.

Perčić, M., Koričan, M., Jovanović, I., Vladimir, N., 2023. Environmental and Economic Assessment of Batteries for Marine Applications: Case Study of All-Electric Fishing Vessels. Batteries 10, 7.

Solutions, S.P.E., 2021. Electrification of ships.

Sui, C., de Vos, P., Stapersma, D., Visser, K., Ding, Y., 2020. Fuel consumption and emissions of ocean-going cargo ship with hybrid propulsion and different fuels over voyage. J. Mar. Sci. Eng. 8, 588.

Tajuddeen, I., Sajjadian, S.M., Jafari, M., 2023. Regression models for predicting the global warming potential of thermal insulation materials. Buildings 13, 171.

The European Committee for Standardization (CEN), 2019. EN 15804:2012+A2:2019 - Sustainability of construction works - Environmental product declarations - Core rules for the product category of construction products.

UN, 2015. ADOPTION OF THE PARIS AGREEMENT - Paris Agreement [WWW Document]. URL ⟨https://unfccc.int/sites/default/files/english_paris_agreement.pdf⟩ (accessed 6.6.24).

UNFCCC, C., 2015. Paris agreement. United Nations Clim. Chang. 1–29.

United Nations Framework Convention on Climate Finance, 2021. Cop26 Sustainability Report.

United Nations Framework Convention on Climate Finance, 2022. COP27 Official Sustainability Report.

United Nations Framework Convention on Climate Finance, 2024. COP28 Report.

Vakili, S., Ölçer, A.I., 2023. Are battery-powered vessels the best solution for the domestic ferry segment? Case study for the domestic ferry segment in the Philippines. Energy 282, 128323.

Wang, H., Boulougouris, E., Theotokatos, G., Zhou, P., Priftis, A., Shi, G., 2021. Life cycle analysis and cost assessment of a battery powered ferry. Ocean Eng. 241, 110029.

Wu, P., Partridge, J., Bucknall, R., 2020. Cost-effective reinforcement learning energy management for plug-in hybrid fuel cell and battery ships. Appl. Energy 275, 115258.

Zahedi, B., Norum, L.E., Ludvigsen, K.B., 2014. Optimized efficiency of all-electric ships by dc hybrid power systems. J. Power Sources 255, 341–354.